1. Introduction

1.1. Hyperspectral/multispectral imaging

Multispectral image is formed by sensors that captures reflected energy within specific band sections of electromagnetic spectrum. Sensors used for capturing multispectral image have between 3 and 10 bands of reflected measurement in every pixel in the image. Sensors belonging to multispectral includes bands belonging to infrared, visible red or green.

Spot, Quickbird,Landsat are commonly used multispectral sensors. Sensors capturing hyperspectral image contains energy in closely related numerous bands than compared to multispectral bands. There are as many as 200 to thousands closely related spectral bands present in hyperspectral imaging. As the bands are very narrowly present they provide spectral measurement in continuous sense over entire electromagnetic spectrum making it more vulnerable or sensitive to any variation in reflected energy. Sensors producing hyperspectral image has much more data contained as compared to multispectral image therefore has greater capability of finding large number of features for example if multispectral image detects forest cover the hyperspectral image can detect up to trees and even species within forest.

The main aim of hyperspectral image acquisition is for obtaining the reflectance curve foe each pixel in an image for identifying materials or objects etc. Materials have unique reflectance value over the entire electromagnetic spectrum known as fingerprint or spectral signatures and characteristic is greatly exploited for identification of material example location of oil fields can be found using spectral signatures of oil.

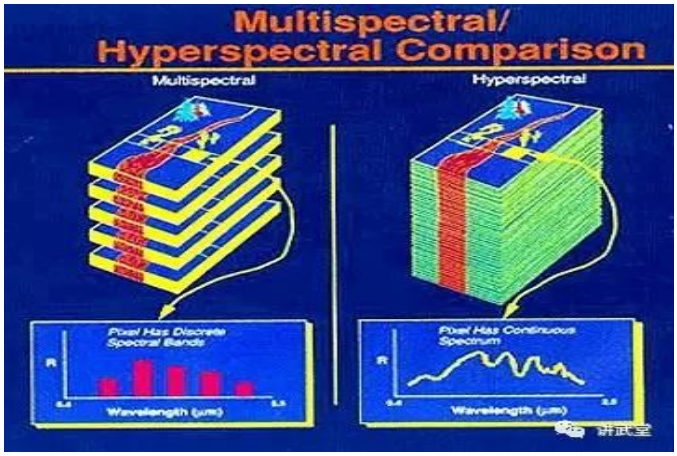

Fig-1

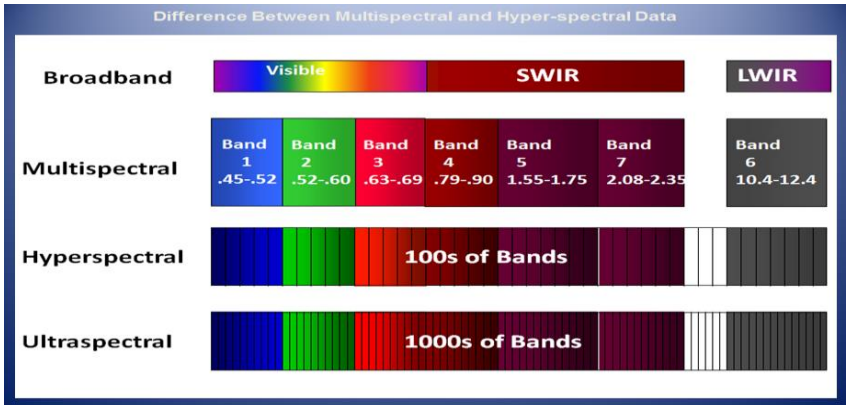

Fig-2

1.1.1. Spectral image basics

For better understanding of hyperspectral imagery lets recall some basic concept that light made up of photon has energy obtained form its wavelength example visible range of light has wavelength belonging from .4 to .7 microns whereas radio waves has wavelength greater than about 30cm.

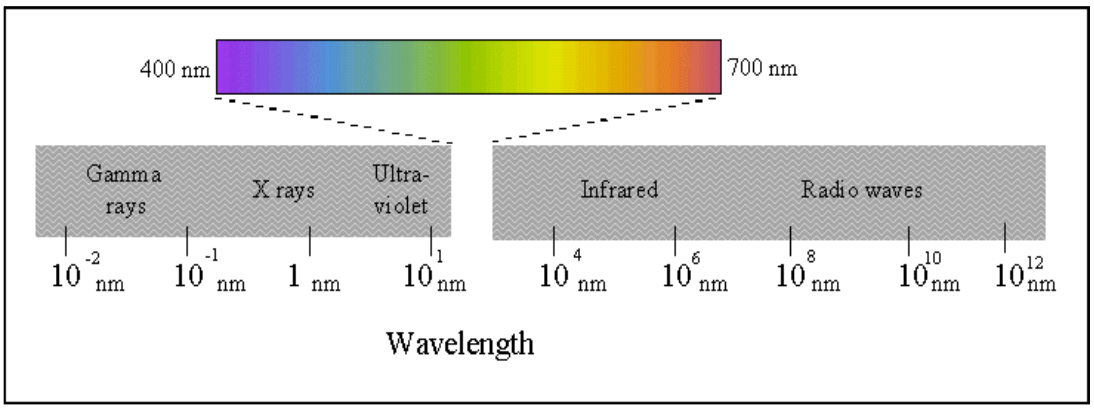

The electromagnetic spectrum

Fig-3

When light falls on any object either it is transmitted, absorbed or reflected, the amount of light reflected back form a material is measured over a range of wavelength known as reflectance spectrum or simply reflectance. This is very important because as the pattern formed due reflectance is unique for unique materials and by exploiting this feature most of the materials can be identified

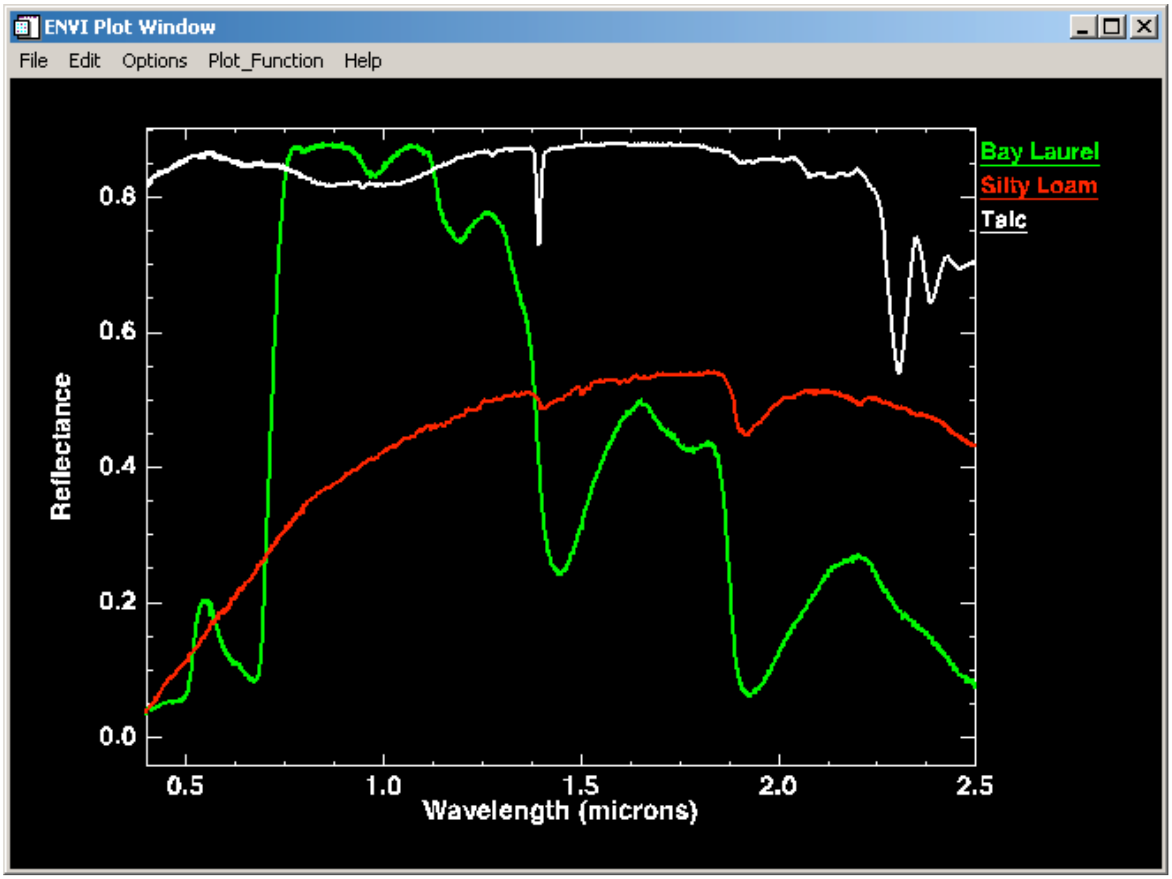

Fig 4

Reflectance of a narrow, closely existing spectral or wavelength bands are usually measured by spectrometers and is plotted in such a fashion that it appears as a continuous curve. Using spectrometer results in recording of reflectance of every pixel present in an image.

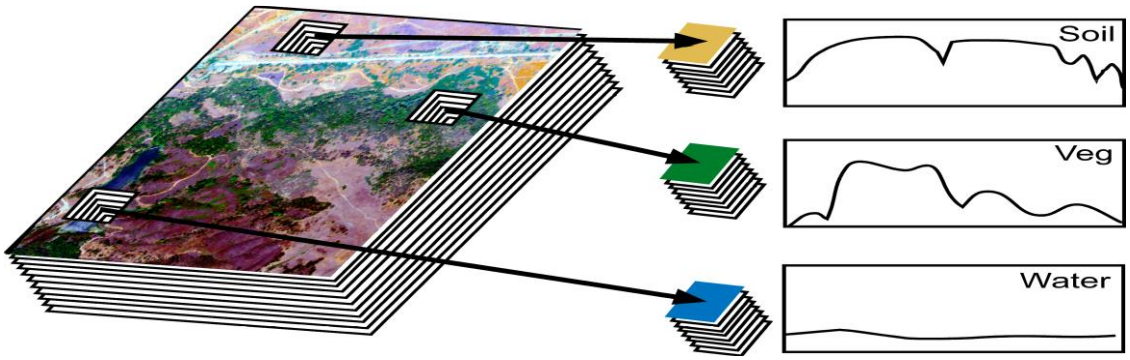

Fig 5

1.1.2. Hyperspectral image sensors

These sensors acquire information in the form of set of images where every image in a set represent narrow range of wavelength in electromagnetic spectrum. Images acquired in this manner are arranged in three dimensional fashion as (x,y,λ) forming hyperspectral data cube Where the spatial coordinates and spectral dimension of the scene are represented by x , y and spectral dimension by λ (i.e wavelength range). Sensors precision is more if the obtained spatial and spectral resolution is high and therefore using high precision sensors only small number of pixels are needed to identify objects. If large pixels are used then multiple objects are captured inside one pixel resulting in increase of difficulty to identify objects and if size of pixel is too small then energy present per sensor cell is deceased which in turn reduces signal to noise ratio and measured features reliability.

1.1.3. Hyperspectral data acquisition

Hyperspectral data acquisition is done mainly four different ways as shown in fig-6

1.Point scan- Light is allowed to fall on a particular point and reflectance curve is recorded pixel wise on to the sensors

2.Line scan- Light is formed in the form of line and reflectance curve of whole line is obtained at once. When this line of light is traversed over entire surface reflectance of entire image is obtained

3.Area scan- Beam of light forms surface and the image is acquired at particular wavelength. If all sets of such image are put together reflectance of entire image is obtained

4.Single Slot- Reflectance of entire image is obtained with a single flash of light.

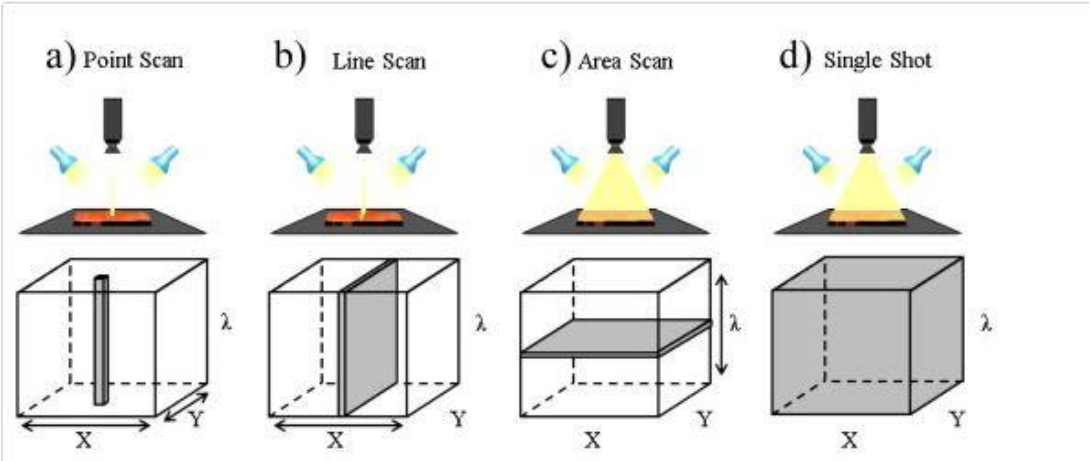

Fig 6

1.1.4 Motivation behind the use of Hyperspectral imagery

Multi-hyperspectral image has very wide and useful range of application using this technology can greatly increase the efficiency and productivity of work. Some of the well-known places where it is already being used are-

Agriculture

Australians are using spectrometer imaging for detecting variety of grapes and developed a warning system that would detect the outbreak of disease in its early stages. Multi-hyperspectral data is used to find chemical composition of crops like nutrients or water etc and then supply them with the deficient data to increase the productivity.

Eye Care

Retinopathy and macular edema diagnosis can be done by the use of Multi-hyperspectral image before causing eye damage

Food Processing

In advanced nut industry, Hyper-multispectral system is installed to separate shells, stones or any alien material from almonds, peanuts, walnuts etc. these systems are also used to separate rotten items form the good ones hence increasing the product quality, lowering reject rates.

Mineralogy

Using spectral matching techniques many important minerals like silica, feldspar, water content, garnet can be detected easily because they have strong spectral signatures.

Environment

Monitoring of hazardous waste released by oil fired, coal or other industries can be done.

1.2. Endmember Detection and class selection

Single pixel of the image may consist of made up of many number of pure spectral footprint or signatures (pure spectral footprints are also known as endmembers), resulting in the presence of mixed pixels in hyper-multispectral image hence spectral unmixing is used to separate mixed pixels in multi-hyperspectral image into their respective abundances and endmembers. Unmixing of endmembers depends upon presence of kind of mixing model. Mixing model may be of linear or nonlinear type which takes into account the shape, size, orientation, atmospheric effect, sunlight angle, sensor material etc. Linear model equation is given as

$$y_i = \sum_{k=1}^{M} x_{ik} e_k + n_i \qquad i = 1, \ldots\ldots\ldots\ldots\ldots N$$

Where y is value of reflectance, e is endmember, x is abundance coefficient and n is the noise present, N is the number of endmember, and M is the total number of pixels present. This model is subject to the condition given as

$$x_{ik} > 0 \ \forall \mathrm{k} = 1, \ldots, \mathrm{M} \qquad \sum_{K=1}^{M} x_{ik} = 1$$

This linear model effectively describes the abundances of the pure material region present in hyperspectral image. Nonlinear mixing model is found to be more efficient in cases where the homogeneous mixing of material is done.

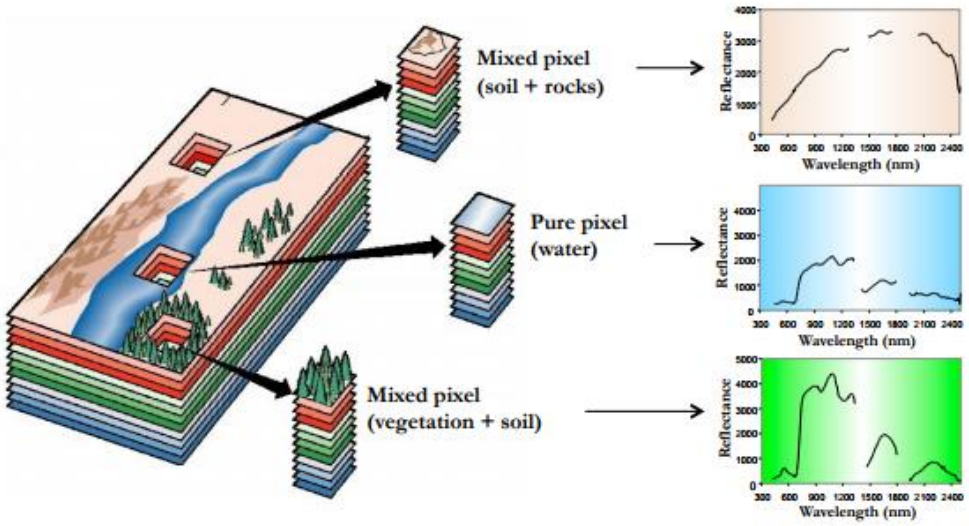

Fig 7

1.3. Band selection

Radiance values of every pixel is calculated over a wide range of wavelength using Multi-hyperspectral sensors results in the generation of heavy amount of data (this is why size of such imagery is very large). Although this large amount of data helps in extraction of material spectra, this increases problems of dimensionality handling, data storage, computational efficiency etc. In order to overcome this problem, use of techniques which results in data reduction with minimum loss of information is inevitable. One such technique is dimension reduction using pca over Multi-hyperspectral is explained and implemented in thesis. The amount of loss of information associated due to dimension is also calculated.

1.4. Problem statement

Multi-hyperspectral unmixing generally requires prior knowledge of the number of endmembers present in the scene and pixel purity assumption which says pure pixel corresponding to each pixel also should exist in the data. Most of the endmember techniques assumes that each pixel of hyperspectral image lies in single region with only one set of endmembers but in reality, single pixel may cover multiple number of endmembers i.e. defining several overlapping regions. Therefore, separation of these endmembers requires very complex iterations and algorithm. In order to select the endmembers for the creation of class to identify materials a simple user guided approach is used in this project in which user identifies the classes by selection of points. These classes are then formed as the basis of classification of material over entire hyperspectral data set.

Hyperspectral data contains large number of spectral bands thus increasing the size of image making it difficult in processing hence techniques are required which can reduce the dimensionality with minimum loss of information.

1.5. Overview of Research

Research conducted in this project involves development of user friendly interface using MATLAB programming language through which the following modules are implemented.

1 Acquisition of hyper-multispectral image and display of its basic properties.

2 Formulation of classes with the help of user selecting points over displayed hyper-multispectral image

3 Reduction of Dimension of hyperspectral image up to user specified number of bands and calculation of the amount of information lost

4. Classification of materials in hyperspectral image through spectral matching using traditional SAS, SDS, SCS approach and displaying the result using windowing technique and enhancing the output using Floyd dithering technique

5 New method proposed for the purpose of material classification over traditional SAS, SDS, SCS approach, (regression transform is used over reflectance curve to obtained separate regression distance class matrix) displaying the result using windowing technique and enhancing the output using Floyd dithering technique

6 obtaining the amount of area classified under each class, processing time, accuracy comparison between traditional and proposed techniques.

2. Literature review

Goetz et al was the first person who introduced the concept of decomposing multi-hyperspectral data into its primary components back in 1985. There are three main steps involves in hyperspectral unmixing. Firstly, identification of spectrally distinct object. second is extraction of its spectral signatures. Third step involves abundance estimation of spectral footprint. Absence of pure pixel and presence of sensor noise, atmospheric noise, mixed background poses difficult challenges for designing model for unmixing of hyperspectral data. In the year 1979 first model for analysing spectral reflectance of the mars data was proposed [1]. A well-known nonlinear model known as **Hapke's model** was proposed in the year 1981 [2]. Handling of non-linear model is very difficult as it includes number of parameters, estimation methods, obtaining fast processing etc. Nonlinear model is often application based [3,4,5]. In [6], for nonlinear unmixing of the hyper-multispectral data geometric distance method is proposed which remained the generalised method for unmixing until the year 1983. Hapke's Linear model [7] was proposed in the year 1983 to unmix mixtures of binary minerals. LMM (Linear mixing model) maps multi-hyperspectral data using affine geometry hence LMM is popularly used in remote sensing areas [8,9,10]. linear stochastic mixing model (SMM) was proposed in the year 1997 [11] by combining spectral clustering with LMM [12]. SMM is a linear model as it incorporated the assumptions proposed in LMM but it also uses probabilistic approach where both endmember footprint and reflectance data are modelled in probabilistic manner rather than deterministic manner as in LMM. In this thesis, we have used spectral distance, spectral angle, spectral correlation and ensemble of all three for the purpose of hyperspectral material mapping [13]. Secondly a new method is also proposed which not only incorporates the SAS, SDS, SCS classifier but also uses regression transform for the generation of regression distance matrix with respect to each class. This means that initially we were having only one reflectance matrix corresponding to particular scene but after using regression transform we have generated as many distance reflectance matrix as the number of classes present for classification. Creation of extra reflectance distance matrix increases the accuracy but also increases the processing time. Effort is also made to enhance the output result by using Floyd dithering technique. Algorithm efficiency can be assessed by error checking between reconstructed reflectance and available reflectance [14].

2.1. Existing hyperspectral image classification technology

1. **Uttam Kumar** proposed hybrid Bayesian classifier [15]. BC assumes that the prior probability of all the class present is equal. Making prior probability equal reduces the accuracy of classification of materials. More improved technique is Hybrid Bayesian classifier which uses High spectral and low Spatial resolution (HSLS) data for the purpose of calculation of class abundance per pixel by unmixing. From this obtained abundance matrix prior probability is calculated, which in turn is used for classification of high spatial high spectral resolution (HSHS) data. [15].

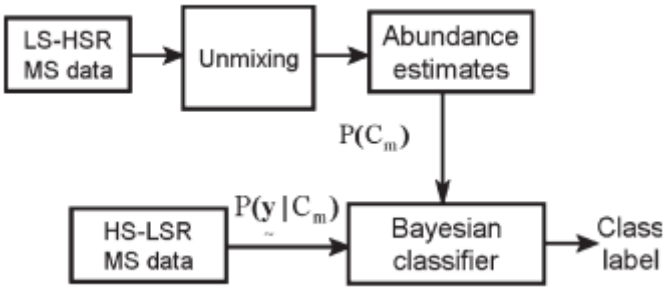

Fig 8

The probability that a particular pattern comes form W_i class is denoted by $p(w_i/x)$. But if the pattern classifier decides that x comes from w_j when it actually came from W_i then loss occurred due to this misclassification is L_{kj}

Average loss occurred is

$r_j(x)= \sum_{k=1}^{W} L_{kj} * p(W_k/x)$.

Applying Conditional probability

$r_j(x)= \sum_{k=1}^{W} L_{kj} * p(x/W_k)p(W_k)$.

Bayes classifier assigns unknown pattern x to w_j if $r_i(x)< r_j(x)$ j=1,2……..W for all $i \neq j$

$\sum_{k=1}^{W} L_{ki} * p(x/W_k)p(W_k). < \sum_{q=1}^{W} L_{qj} * p(x/W_q)p(W_q).$ for all $i \neq j$

Loss function L_{kj} = 1-β_{ij} where β_{ij} =1, if i=j, & β_{ij} = 0 if $i \neq j$

$r_j(x)= \sum_{k=1}^{W}(1-\beta_{ij}) * p(x/W_k)p(W_k)$

equivalently $p(x/W_i)p(W_i)> p(x/W_j)p(W_j)$ j=1,2……..W

now a distance parameter is defined for 2-D case as

$d_j(x)= p(x/W_i)p(W_i)$

probability density function is assumed to be Gaussian distribution then the distance parameter is given as

$d_j(x)=1/\frac{1}{\sqrt{2\pi\sigma}}\, e^{\frac{-(x-m_j)^2}{2{\sigma_j}^2}} * p(W_i)$ j=1,2

similarly, this can be extended to n dimensional case of hyperspectral data as

$$p\left(\frac{x}{W_j}\right) = \frac{1}{n/2\sqrt{2\pi}} * \frac{1}{|C_j|^{1/2}} e^{-(x-m_j)'C_j^{-1}(x-m_j)}$$

Where $m_j = E\{x\} = \frac{1}{N_j}\sum_{x\varepsilon W_j} x$

$$C_j = E\{(x-m_j)(x-m_j)'\} = \frac{1}{N_j}\sum_{x\varepsilon W_j} x\,x' - m_j m_j'$$

Taking logarithm and the dropping of the constant terms and independent terms equation reduces to

$d_j(x)=\ln[\, p(x/W_j)p(W_j)\,]$

$$\mathbf{d_j(x)= \ln p\left(\frac{x}{W_j}\right) + x'C^{-1}m_j - .5 * m_j'C^{-1}m_j}$$

based on the above distance Bayesian classification is done. This value of distance is calculated with respect to spectral footprint and target pixel reflectance. Smaller the value of Bayesian classifier distance larger the similarity is present. In [15] Bayesian classification and hybrid Bayesian classification is used and the average efficiency obtained is 76% and 86% respectively

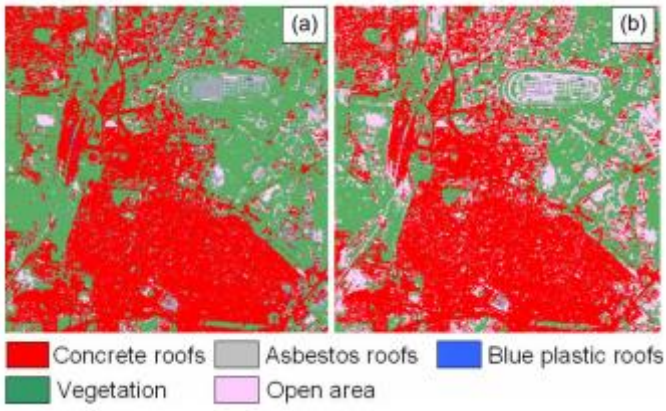

Fig- 8-Bayesian classifier. (b) HBC

2. **B. Krishna Mohan.et.al.in** [16] in the year 2015 proposed a way of dealing with the difficulty present in processing of hyperspectral data. Difficulty includes presence of redundant information, high volume of data because of multidimensional matrix of image. In [16] presented a framework for dealing with hyperspectral imagery which included reduction of atmospheric noise, reduction in dimension and imagery classification. Mixture modelling phenomenon is also explained, followed by a recent development in mapping the classes at sub-pixel level based on the principle of super resolution

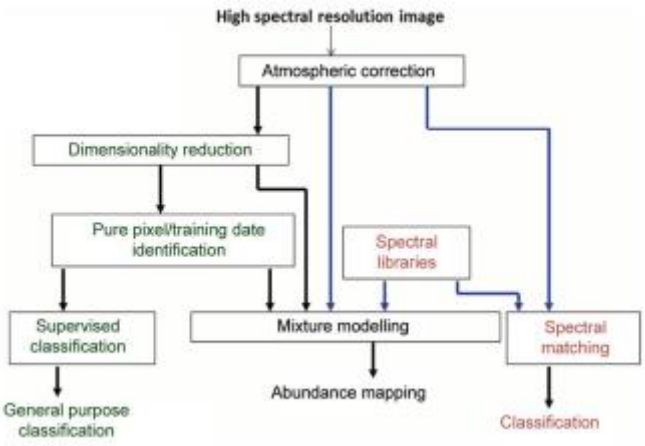

Fig 10

B. Krishna Mohan classification average accuracy of 92% and kappa coefficient of .8 is evaluated for the image using 155 bands.

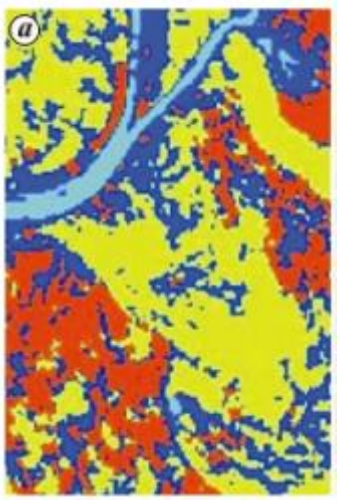

Fig 11

a. Classification of original 30 m resolution Hyperion image is done for water, vegetation, land, and build ups.

3. **Saeid Homayouni** proposed in [17] a material mapping method which can be considered as multi step target detection. The strategy used is similarity measurement which is of two types generally i.e. stochastic measures and second is deterministic measures. This paper tests deterministic measures of hyperspectral data. Similarity is measured by calculating Euclidian distance (Ed), spectral Pearson correlation (SC), spectral angle (SA), spectral similarity value (SSV) for the purpose of finding the pixels having most similar object of interest. In order to incorporate benefit of every spectral similarity classifier and reject the weak points fusion technique is used.

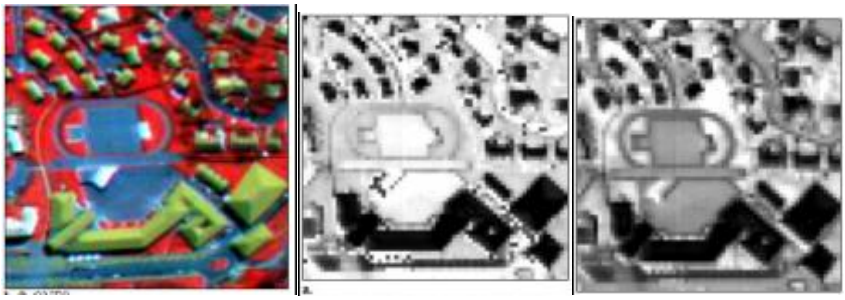

Fig 12

a. 48 band hyper image b.ssv similarity c. sas similarity

Saeid Homayouni classification average accuracy of 96% and kappa coefficient of .86 is evaluated for the image using 48 bands.

4. Naveed Akhtar proposed [18] reflectance measured by multi-hyperspectral sensor of a mixed pixel contains combination of many materials on the ground. He proposed a technique for calculation of fractional abundance of endmembers. He proposed greedy sparse method over sparse method for the purpose of unmixing of endmembers and abundance matrix calculation. Greedy algorithms accuracy is highly sensitive to the presence of high correlation of reflectance of different materials. To deal with this shortcoming the proposed greedy sparse approx. algo.(SUnGP) for the purpose of unmixing of multi-hyperspectral data. SUnGP showed good response against the correlation of reflectance of materials. subspace pruning technique is used for endmember identification. This method has a comparable accuracy to the methods using convex relaxation with increased processing advantage.
   Sparse unmixing is performed on data obtained from [19]. Dimension of image 350 × 350 × 224. This image represents the region of alunite, Culprits mine, Nevada. SUnGP algorithm estimated the pixels region which are having high abundance of alunite, Cuprites minerals present. The have provided result only for the visual comparison [20] [21]. Real word data is used so quantitative analysis is not possible because of the absence of ground truth data availability.

5. **Jun Li, Xin Huang** in the year 2015 proposed in [22] that single type of feature can be extracted by the use multiple kernel learning or composite kernel model. He developed few methods to integrate multiple features extracted from nonlinear and linear transformations. In [22], introduced a new method for classification of multiple feature.
   A major characteristic of the developed approach is that it does not require any regularization parameters to controlling the weights of exploited features so that different types of features can be effectively integrated in a flexible and collaborative way. The overall average efficiency calculated for Pavia centre data [23] is around 92%.

3. Methodological Approach

Classification of endmembers are done mainly in two ways deterministic approach and probabilistic approach. This thesis deals with unmixing model in deterministic method. To deal with massive amount of data present in hyperspectral imagery, technique for the reduction of dimension of hyperspectral image using pca is implemented on MATLAB. A separate module has been designed in MATLAB using graphical user interface which can reduce the dimension of the data up to the wish of the user and accordingly also calculates the amount of information. Another module is designed with the help of MATLAB which uses the deterministic approach of similarity measurement like SAS, SDS SCS Classifiers for the purpose of unmixing of endmembers.

This thesis proposes an improvement in the deterministic approach of similarity measurement like SAS, SDS SCS Classifiers for the purpose of unmixing of endmembers.

Improvement in classification is done by applying regression transform to the spectral reflectance of the hyperspectral data. Details of the new method proposed is explicitly explained in this thesis. Proposed method shows improvement in results visually and quantitatively. Windowing technique is also implemented for the purpose of making output more visually effective. This technique is implemented in user interactive way such that user can select the size of window to achieve best visual result possible. Another module is also designed which gives the number of pixels points classified per class and amount of area covered by pixels belonging to same class, processing time of each algorithm is also calculated in this module for processing time comparison.

3.1. Review of SAS, SCS, SDS classifiers

We are considering multi-hyperspectral image as cube of matrix data, then every pixel is an observation vector

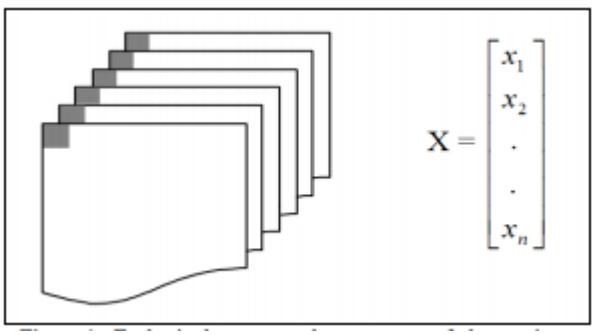

Fig 13-Each pixel corresponds to a vector of observations

3.1.1 Spectral Distance Similarity (SDS)

Here the similarity distance is defined as $\boldsymbol{d_{sds} = \sqrt{(\sum_{i=1}^{n}(t_i - x_i)^2)}}$

Where t_i is the target pixel vector, x_i is the hyperspectral data pixel vector. For the purpose of normalization of values between 1 and 0

$$\boldsymbol{d_{norsds} = \frac{d_{sds} - m}{d_{sds} - M}}$$

Where M and m are maximum and minimum values d_{sds} respectively.

3.1.2. Spectral Correlation Similarity (SCS)

Statistical Pearson coefficient σ is used as similarity measurement, shows correlation between two vectors and is defined as

$$\boldsymbol{\sigma = \frac{1}{n-1}\left(\frac{\sum_i^n (t_i - \mu_t)(x_i - \mu_x)}{\sigma_t \sigma_x}\right)}$$

where σ and μ are standard deviation and mean of pixel and target vector respectively.

Reflectance similarity value is obtained by combining the Euclidian distance and correlation similarity+

$$\textbf{RSV}=\sqrt{(d_{sds}{}^2 + (1 - \sigma^2))}$$

Similar vectors have identical direction and magnitudes. Average reflectance i.e. brightness corresponds to magnitude and spectral shape corresponds to direction. Both of this factor must be quantified while drawing similarity of two spectra. Shape is compared by using correlation and RSV combines shape and brightness having a maximum of square root of two and minimum of zero. Smaller the value of RSV larger is the similarity between the two-reflectance curve.

3.1.3. Spectral Angle Similarity (MSAS)

hyper-angle calculated as given

$\boldsymbol{\alpha = \arccos\left(\frac{\sum_{i=1}^{n} x_i t_i}{\sqrt{(\sum_{i=1}^{n} t_i{}^2)}\sqrt{(\sum_{i=1}^{n} x_i{}^2)}}\right)}$ smaller the angle more is the similarity between target spectra and pixel vector.

3.1.4. ALGORITHM

STEP 1- Load hyper-multispectral image.

Get [m,n,p]=size(image) % dimension calculation

STEP 2- Load signature reflectance of material for spectral reflectance matching of the material.

STEP 3- to get to reflectance value per pixel, per wavelength

for i=1 to row

for i=1 to col

for j=1 to bands

calculate distance between target pixels reflectance and signature pixels reflectance with respect to each class

$$d_{sds} = (reflectance\_value(i,j,k) - signature\_reflectance(k)^2)$$

STEP 4 -SAS calculated using

$$\alpha = \arccos\left(\frac{\sum_{i=1}^{n} x_i t_i}{\sqrt{(\sum_{i=1}^{n} {t_i}^2)}\sqrt{(\sum_{i=1}^{n} {x_i}^2)}}\right)$$

Step 5- SCS calculated using

$$\sigma = \frac{1}{n-1}\left(\frac{\sum_{i}^{n}(t_i-\mu_t)(x_i-\mu_x)}{\sigma_t \sigma_x}\right)$$

Lesser is the distance more is the similarity

STEP 6- Applying Fusion/Ensemble Strategy

Initialize matrix of same size(row and col) call it ensemble matrix=zeros

Ensemble matrix is used to hold certain quantized value depending upon the class identified.

STEP 7- (0,0,0) shows pixel favoured by no class.

(0,0,0) shows pixel favoured by no class.

(1,0,0) shows pixel favoured by SDS Classifier only.

(0,1,0) shows pixel favoured by SAS Classifier only.

(0,0,1) shows pixel favoured by SCS Classifier only.

(1,1,1) shows pixel favoured by SCS, SDS, SAS Classifier.

STEP 8- Target pixel is assigned to that class which is favoured by more than one classifier.

STEP 9- Windowing technique is used to enhance the result.

STEP 10- END

3.1.5. FLOWCHART

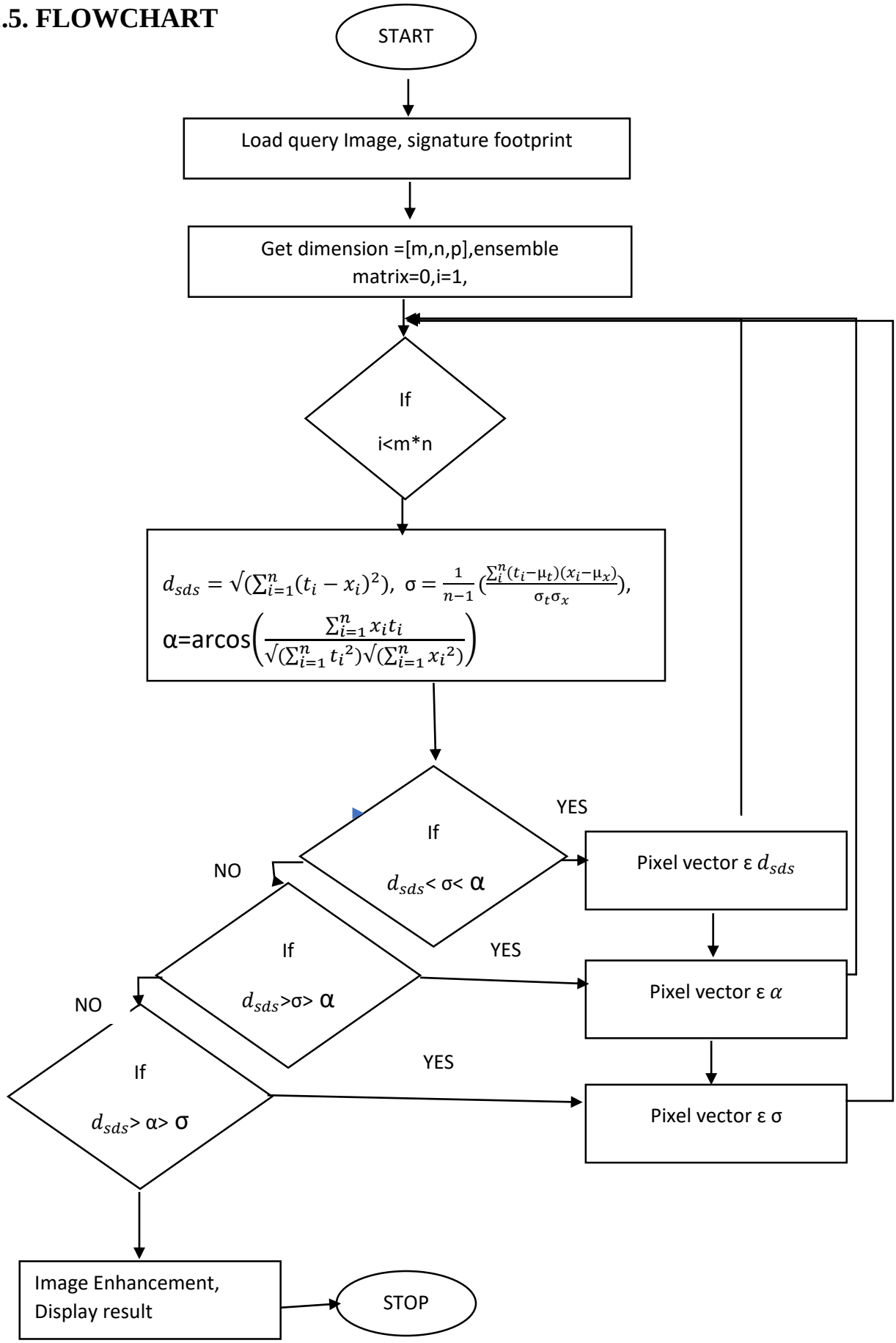

3.2. Hyer-multispectral dimension reduction using principal component analysis.

Review of principal component analysis

Hyperspectral data are highly correlated so there is scope of dimension reduction while preserving variations of features present in the data. Pca transforms data from on dimension to other orthogonal dimension, ordered such that the retention of variation present in the original variables decreases as we move down in the order. First pca has maximum variations or maximum information present in original component. the eigenvectors of a covariance matrix are the pca. Since the covariance matrix is real and symmetrical pca is orthogonal.

Intuitively, pca can give a lower-dimensional picture, a shadow or projection of this object when viewed from its most informative viewpoint.

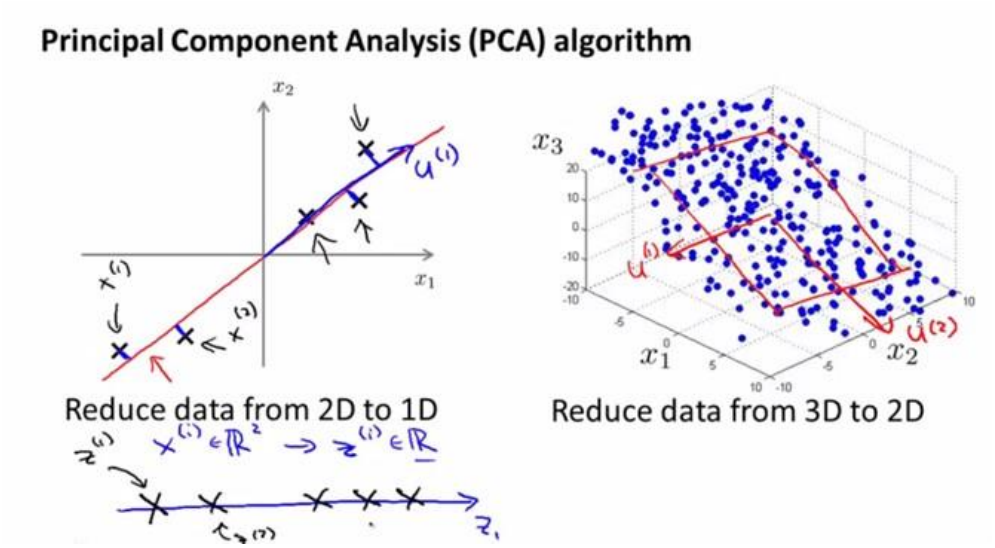

Fig 14.1

3.2.2. Implementing PCA on a N-D Dataset algorithm

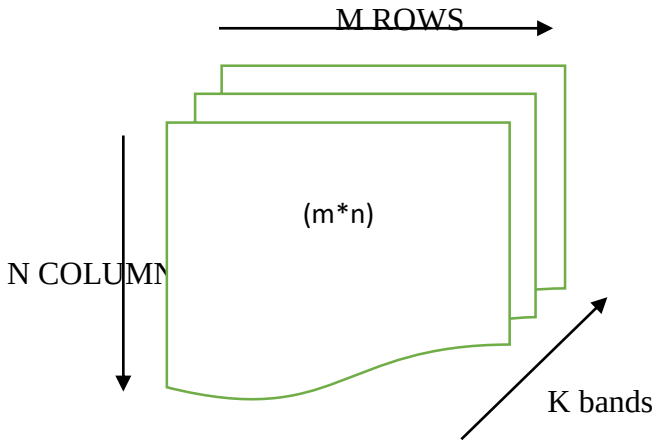

Fig14.2-Hyerspectral data matrix

STEP 1- Load query image, obtain dimensions=[m,n,p]

STEP 2- convert m X n X p dimensional data to a (m*n) X p dimensional data.

Initialize i=0; For j=1 to m

For j=1 to n

Increment i by 1

2D reflectance(:,i) = 3D reflectance(j,k,:)

End ; End

STEP 4- Mean calculation as $m_x = \frac{1}{k}\sum_{k=1}^{1} x_k$

STEP 5-Covariance calculation as

$$C_j = E\{(x - m_j)(x - m_j)'\} = \frac{1}{N_j}\sum_{x\varepsilon W_j} x\, x' - m_j m_j'$$

Covariance matrix is real and symmetrical therefore n orthogonal eigen values possible

Let $\lambda_1 > \lambda_2 > \lambda_3 > \lambda_4 > \lambda_5 > \cdots \ldots \ldots \ldots \ldots \ldots \ldots \lambda_n$

STEP 6 - V be eigen vector matrix, D be the eigen value matrix of covariance matrix. Rows of V corresponds to eigen vector. D be the diagonal matrix consisting of eigen values in decreasing order

STEP 7-Transformation given as equation below also known as Hotelling transform

$y = \mathrm{A}(x - m_x)$

$V^{-1} = V'$ V be orthogonal vector matrix

STEP 8- To reduce dimension eigen vector corresponding to lower value eigen values are eliminated and the inverse reconstruction is given as

$\mathrm{x} = (V'y + m_x)$

reconstruction after dimension reduction given as

$\dot{\mathrm{x}} = (\tilde{\mathrm{V}}y + m_x)$ $\tilde{\mathrm{V}}$ is reduced eigen vector matrix

$\dot{\mathrm{x}}$ is reconstructed matrix

STEP 9- conversion of 2-D matrix to 3-D matrix using inverse of step-2.

STEP 10- Loss of information due to reduction in dimension is given as

$$L_{info} = \sum_{t=1}^{n} \lambda_t - \sum_{j=1}^{k} \lambda_j$$

$$= \sum_{i=k+1}^{n} \lambda_i$$

STEP 11- END

3.2.2. FLOWCHART

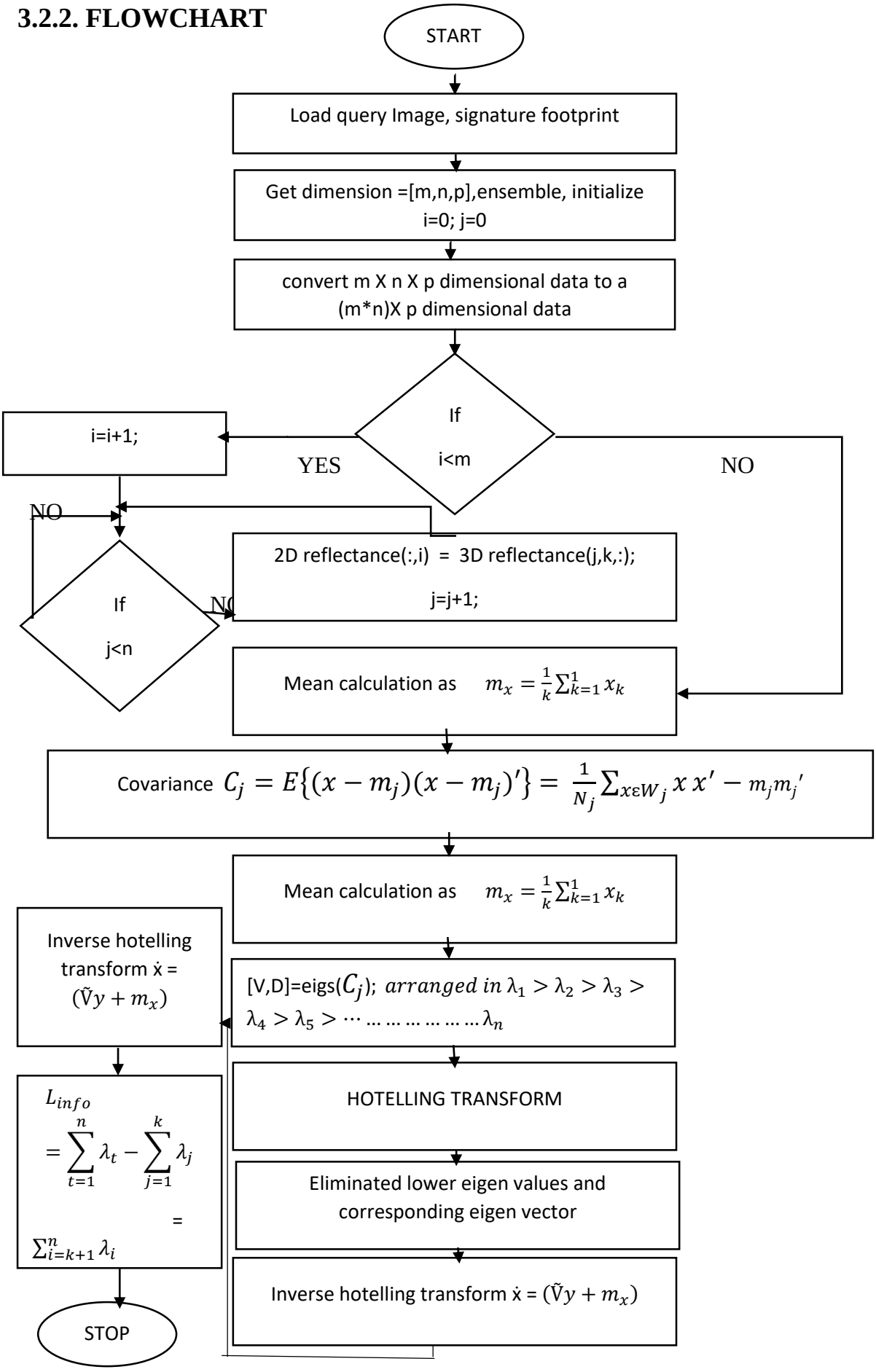

3.3.1. Review of regression algorithm

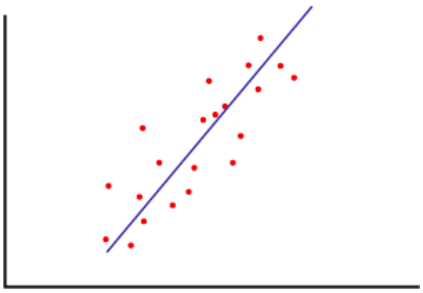

Model representation

Notation

M=number of tanning examples

$x's$ = Input features/variables

$y's$ = output features/ target variables

(x,y) = training example

$(x^{(i)}, y^{(i)})$ = i^{th} training example

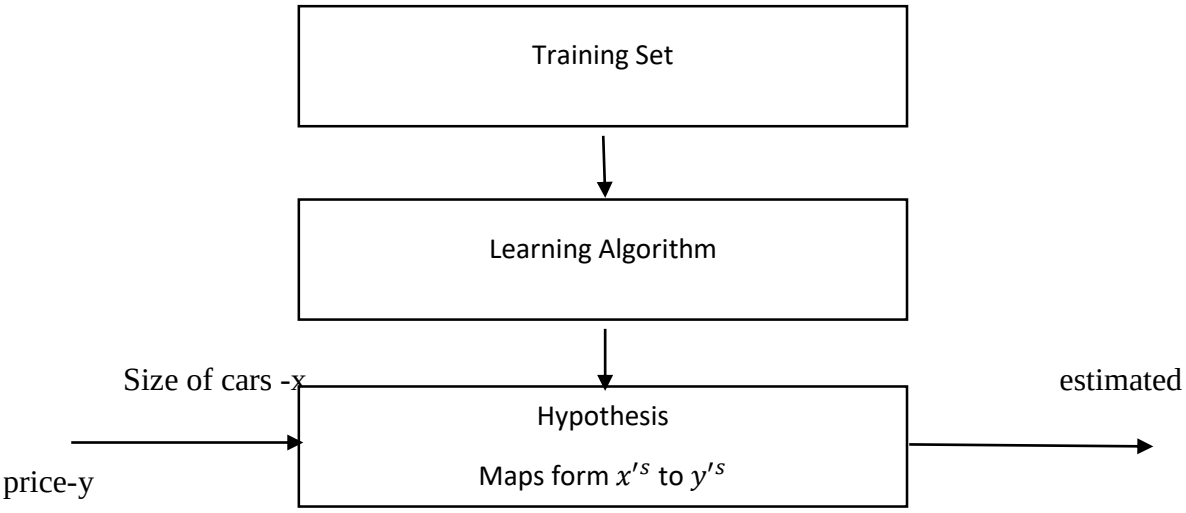

Hypothesis: $h_{\emptyset}(x) = cx$

This model also called univariable linear regression.

Cost Function: J ($\emptyset_0, \emptyset_1$)

How to fit best possible line to our data

Hypothesis $h_{\emptyset}(x) = \emptyset_0 + \emptyset_1 x$ $\emptyset_i's$ $parameter$, m is number of samples

Choosing $\emptyset_i's$, such that $\emptyset_0, \emptyset_1$ of $h_{\emptyset}(x)$ is close to y for training examples

$minimize_{\emptyset_0,\emptyset_1} = \frac{1}{2m}\sum_{i=1}^{m}(h_{\emptyset}(x^i) - y^i)^2$

3.3.1. Algorithm of regression transform on hyperspectral image

Explanation of this new technique is done in steps and visually for easy and clear understanding of algorithm.

x_i→value of i^{th} pixel

i =1 to k → no of bands present in hyperspecral imagery

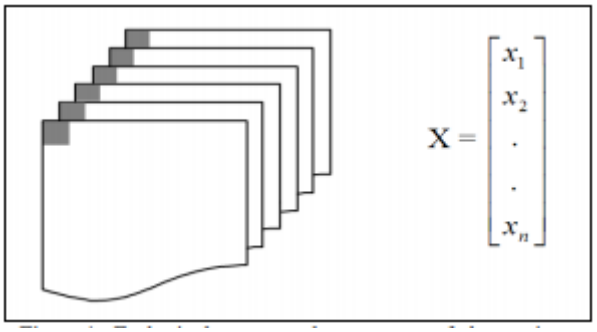

Initially SAS,SDS,SCS Classifier directly uses the reflectance value of hyperspectral for classification. Here, new method is proposed that first transform or project data through regression technique into the new domain. This method is explained in steps below.

STEP 1- Obtain the signature reflectance curve for a perticular range of spectra.

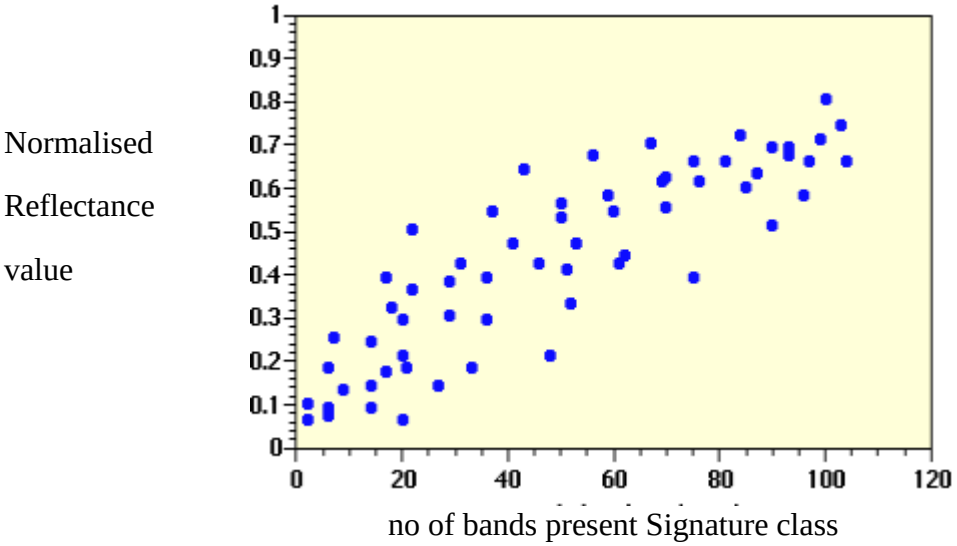

STEP 2- Apply regression technique to find out the best fit line through reflectance curve

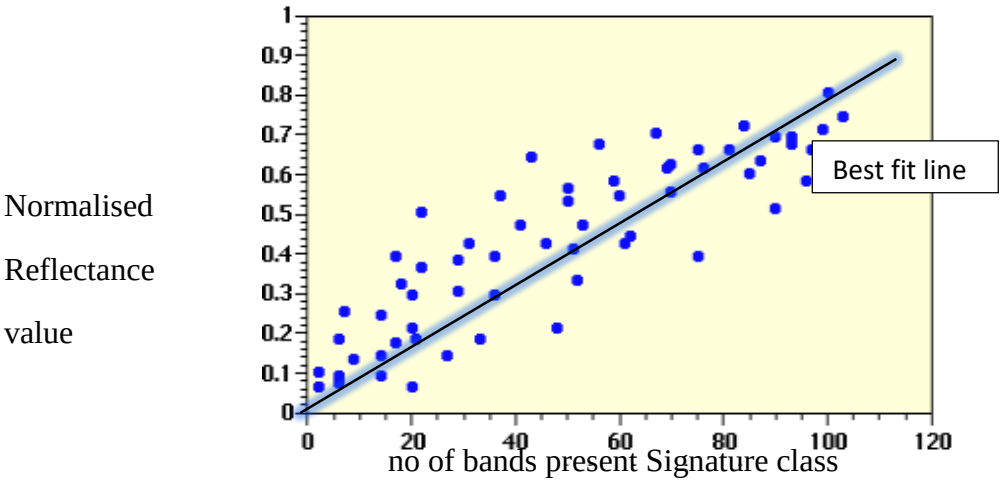

STEP 3- Obtain the perpendicular distance from each reflectance value to the line

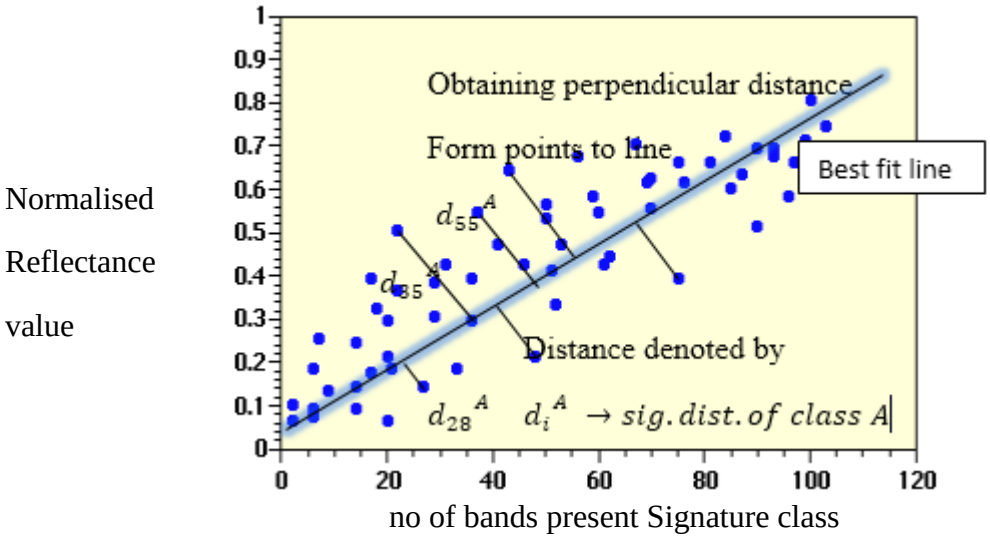

STEP 4- Step 3 creates **regression reflectance distance** matrix and is denoted by d^A

$$d^A \rightarrow \left[d_1{}^A, d_2{}^A, d_3{}^A, \ldots\ldots\ldots\ldots\ldots\ldots\ldots d_i{}^A\right] \qquad i = no\ of\ bands$$

STEP 5- Perform step 1,2,3,4 for all signature class present for classification

STEP 6- Take test vector reflectance curve and superimpose best fit lines obtained from each Signature class over the test pixel vector. Obtain the perpendicular distance from each reflectance value to each superimposed line of characteristic class.

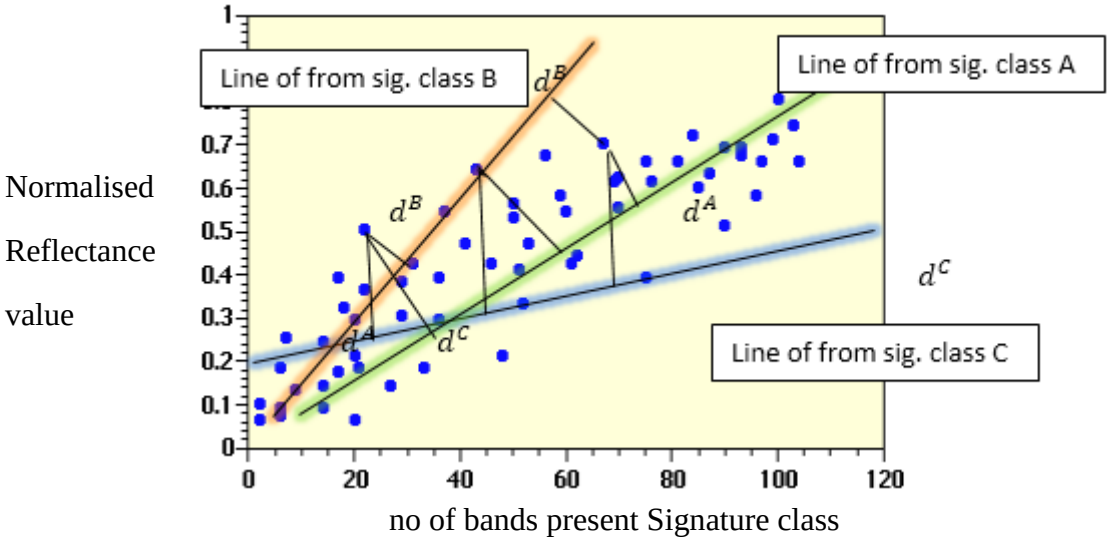

STEP 7- STEP 6 Leads to the creation of as many distance regression reflectance matrix as the number of class present for classification. Example for three class used.

$((d_i{}^{AT})_{m*n*k}), ((d_i{}^{BT})_{m*n*k}), ((d_i{}^{CT})_{m*n*k})$

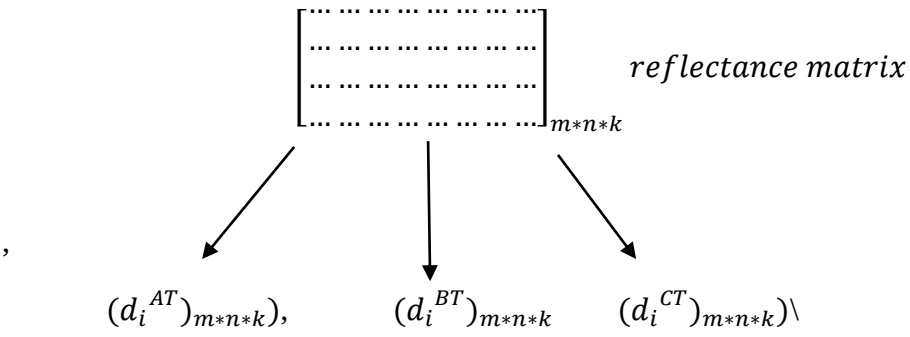

,

$(d_i{}^{AT})_{m*n*k}),$ $(d_i{}^{BT})_{m*n*k}$ $(d_i{}^{CT})_{m*n*k})\backslash$

Advantage of above steps-

- Increases resolution
- Increases the minute variations which are now more detectable. Previously these variations were not detected by the same classifier used. This is proved by both visual and qualitatively results.
- Increases resolution as every signature class has now its own distance reflectance curve for classification
- Increases signal to noise ratio.
- Increases accuracy of algorithm

Disadvantage

- Extra functions added increases processing time

STEP 8- For every pixel use classifier SAS, SDS, SCS and fusion techniques.eg for i^{th}pixel in $(d_i{}^{AT})_{m*n*k}$ use d^A as signature class. Similarly apply for other classes also and calculate similarity index with the help of classifier used.

STEP 9 - $d_{sds} = \sqrt{(\sum_{i=1}^{n}(t_i - x_i)^2)}$

$$\sigma = \frac{1}{n-1}\left(\frac{\sum_i^n (t_i-\mu_t)(x_i-\mu_x)}{\sigma_t \sigma_x}\right),$$

$$\alpha=\arccos\left(\frac{\sum_{i=1}^{n} x_i t_i}{\sqrt{(\sum_{i=1}^{n} {t_i}^2)}\sqrt{(\sum_{i=1}^{n} {x_i}^2)}}\right)$$

STEP 10- Similarity index value is large then similarity between the curve is very less.

STEP 11- Ensemble technique + windowing technique

STEP 12 End

3.2.2. Flowchart

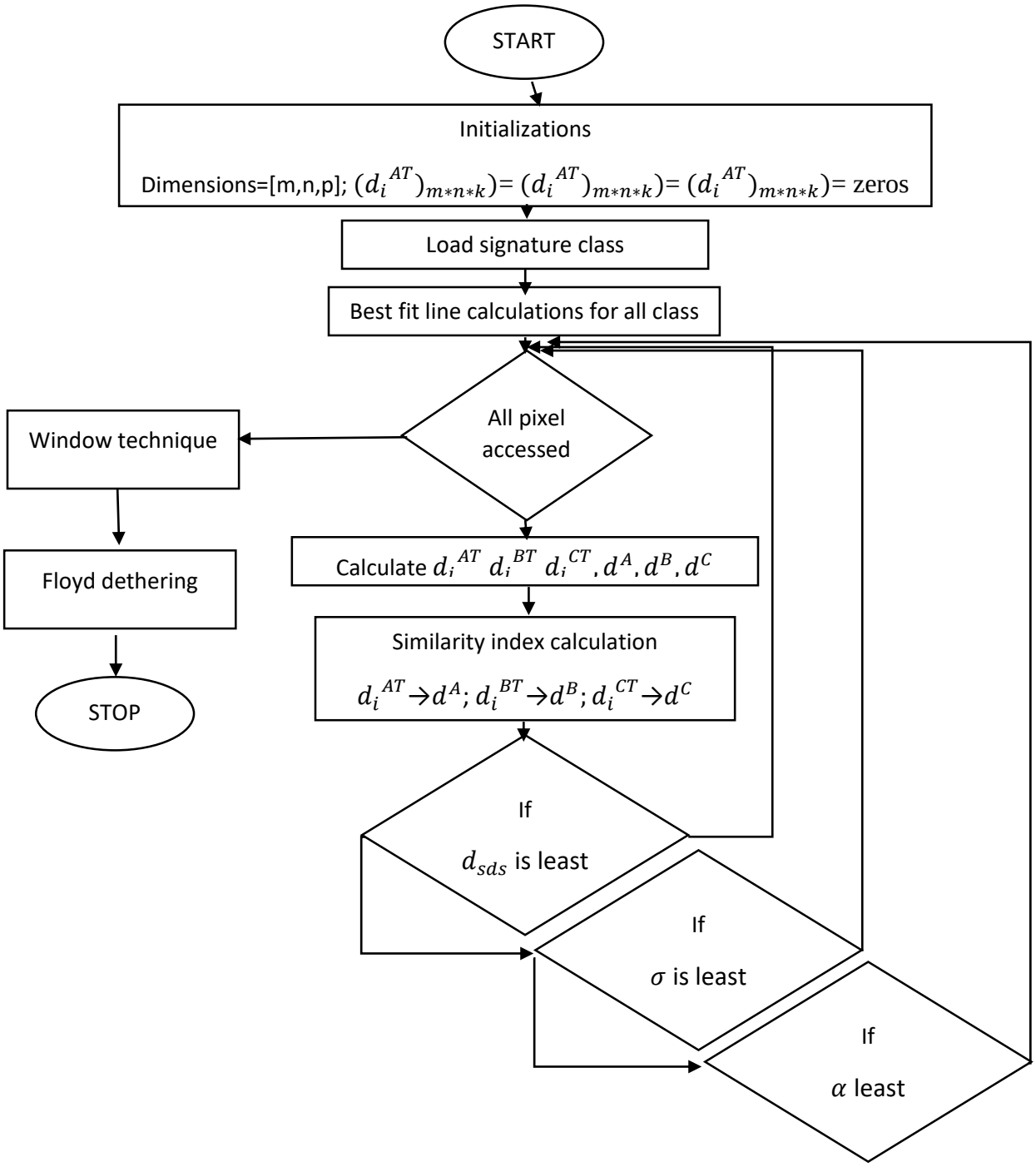

3.4. Windowing technique

Pixel wise display causes each pixel to be classified in any of A,B,C class that leaves final output unrecognized to human eye. Visual result is not available. Windowing technique is actually image enhancement technique that makes data recognizable. In this project windowing technique is implemented in a way that user can give the size of window he wishes to apply and choose the result accordingly.

This technique is explained with the help of example

Let A, B, C are the classes identified using above proposed algorithms. Matrix given below represents output of the classifier in which a hyperspectral image has been classified into three classes. Each pixel of hyperspectral image would be classified as shown below.

A	B	B	C	A	B
A	C	A	B	C	C
B	B	A	A	A	C
C	C	B	C	B	C
A	A	C	C	A	A
A	B	B	A	A	A

Fig 15

If take window of size two

Start translating this window over Image matrix such that the whole image is covered atleast once by above choosen window size. What majority lies in window while it is superimposed on image, whole pixel of the image is assigned same value as shown below in Fig-

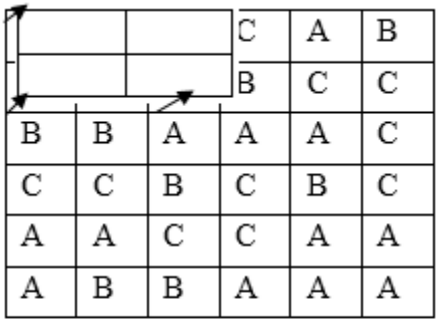

A	B
A	C

Fig 16

According to the majority rule the image matrix now become as shown in fig-17 and window is moved to new position. This process is carried over to entire image.

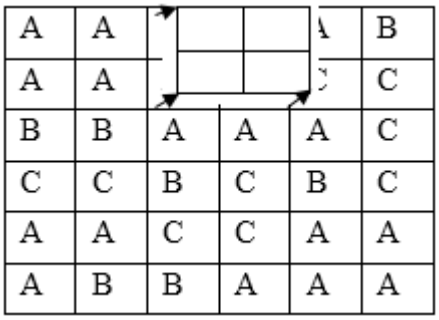

Fig-17

As the window size is increased image smoothness increases but accuracy with which image was classified decreases. Therefore, window technique is only used to get visually results and not in quantitative result where accuracy is of paramount importance.

4. Results

Graphical user interface display and module explanation.

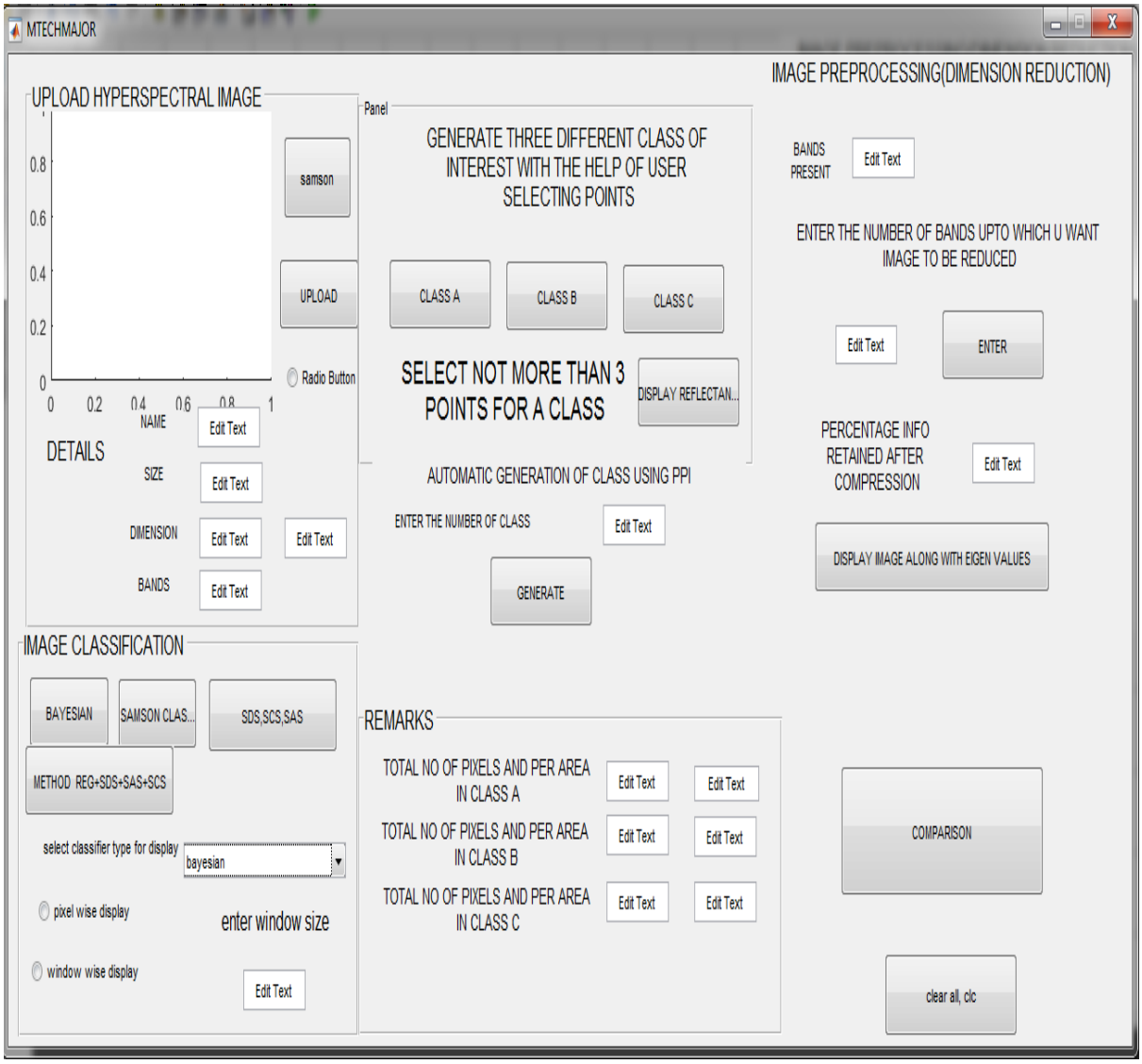

Fig-18

Module 1- Acquisition of hyper-multispectral image and display of its basic properties.

Module 2- Formulation of classes with the help of user selecting points over displayed hyper-multispectral image. For the images in which signature reflectance library is already available user help for the selection of spectral signature is not required.

Module 3- Reduction of Dimension of hyperspectral image up to user specified number of bands and calculation of the amount of information lost.

Module 4- Material class mapping by reflectance Matching of hyper\multispectral image using traditional SAS, SDS, SCS approach and displaying the result using windowing technique and enhancing the output using Floyd dithering technique. New method proposed for the purpose of material classification over traditional SAS, SDS, SCS approach ,(regression transform is used over reflectance curve to obtained separate regression distance class matrix) displaying the result using windowing technique and enhancing the output using Floyd dithering technique

Module 5- This part calculates the number of pixels, amount of amount of area classified under each class, processing time, accuracy comparison between traditional and proposed techniques.

4.1. Class selection

If signature spectral library is not available then this part helps in extraction of spectral signature with the help of user selecting points as shown in fig-19,20,21

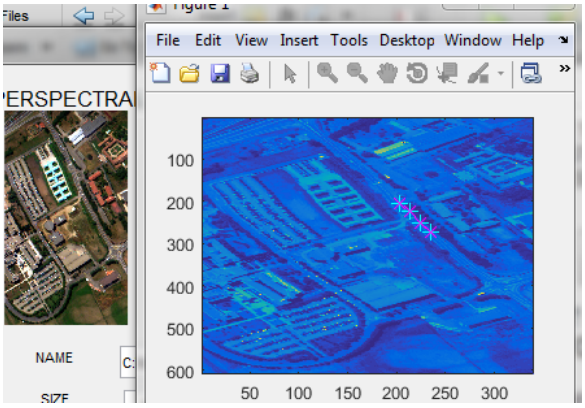

Fig19- selection of roads.

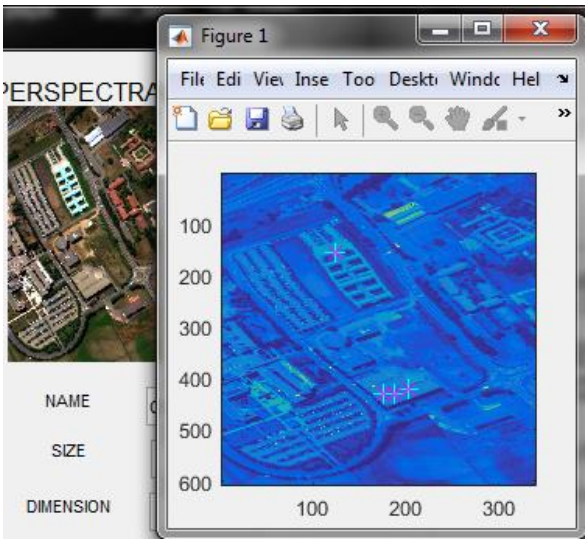

Fig 20- selection of rooftops.

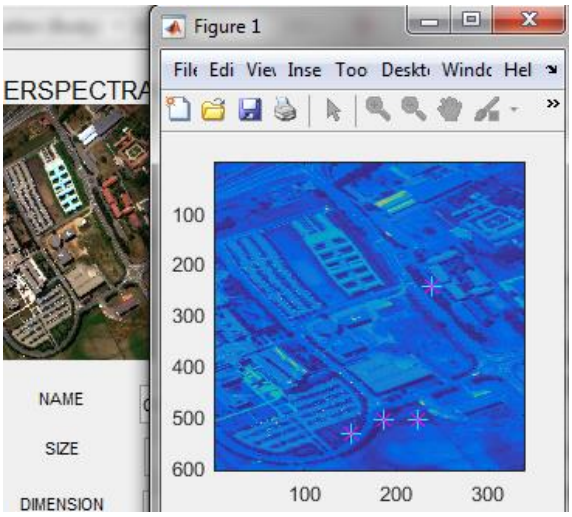

Fig-21 selection of plantations.

Display of the reflectance curve of selected road, rooftops and plantations

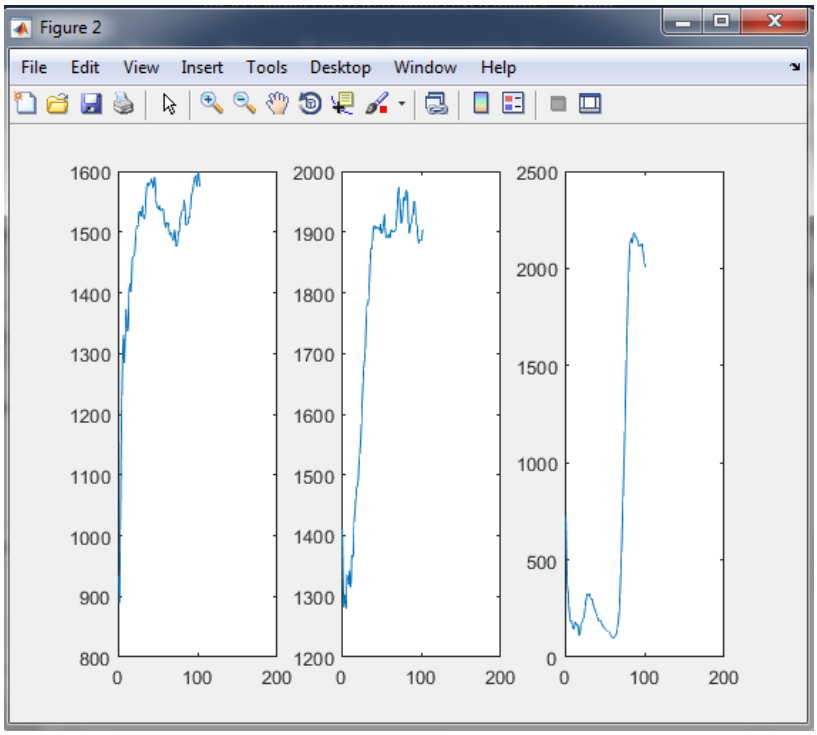

Fig-22

4.2. Band reduction result

Configuration used- Core i5, RAM 2 GB, 2 GHZ processor

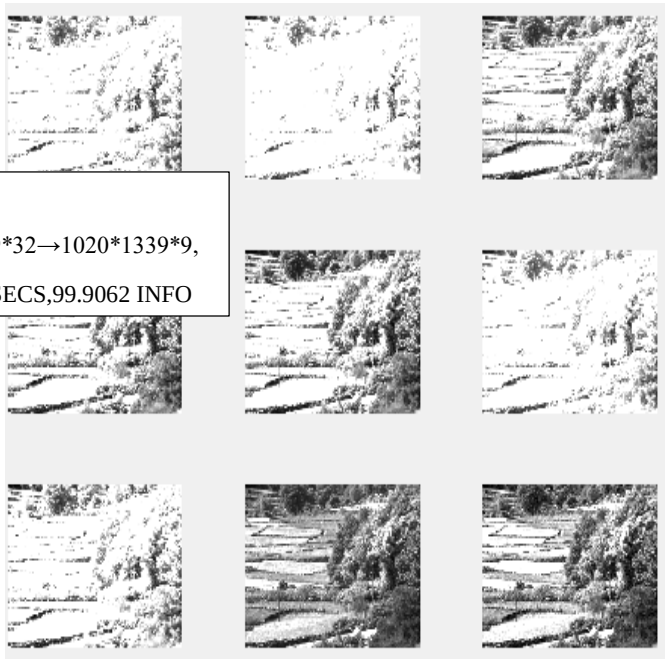

192 MB.
1020*1339*32→1020*1339*9,
156.3785 SECS,99.9062 INFO

Fig-23

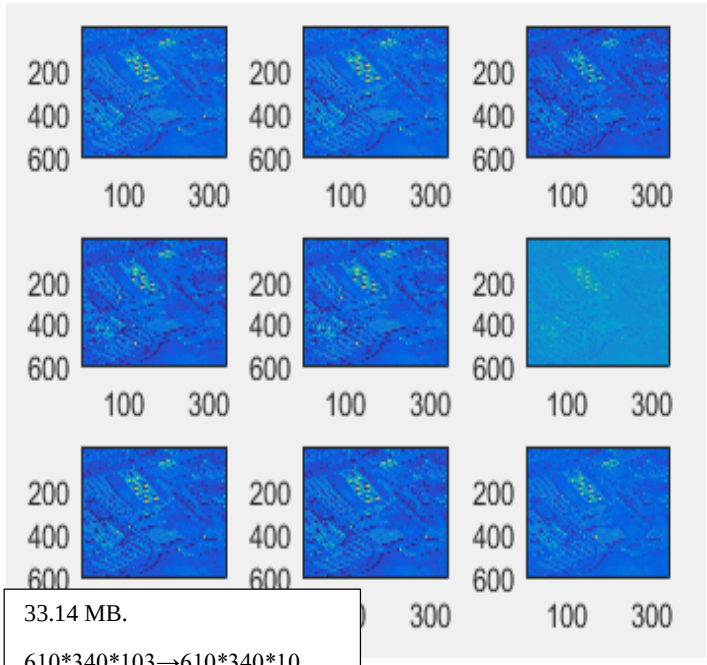

33.14 MB.
610*340*103→610*340*10,
29.5266 SECS,99.6442 INFO

Fig-24

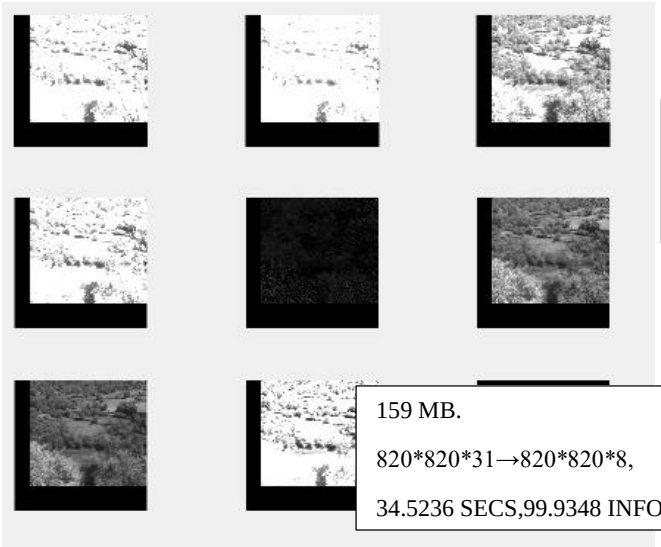

159 MB.
820*820*31→820*820*8,
34.5236 SECS,99.9348 INFO

Fig-25

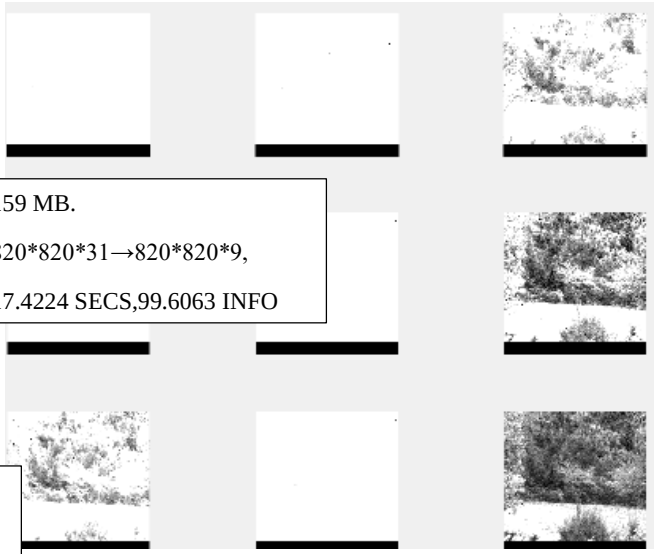

159 MB.
820*820*31→820*820*9,
17.4224 SECS,99.6063 INFO

Fig- 26

4.3. Classifier results

Test images used is downloaded from [24] and [25].

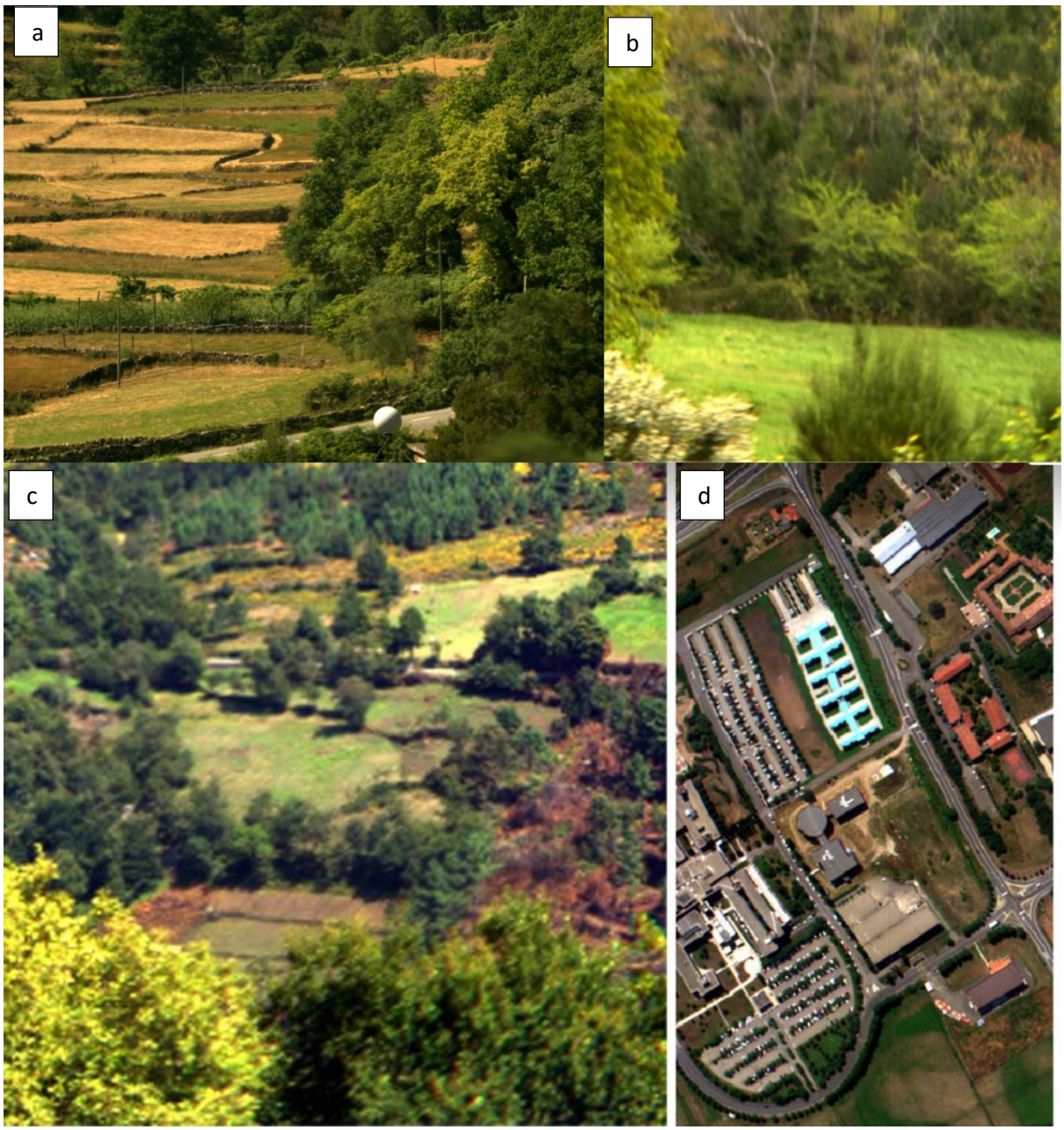

Fig-27

a) Used in test result 1 b) Used in test result 2 c) Used in test result 3 d) Used in test result 4

Test result 1

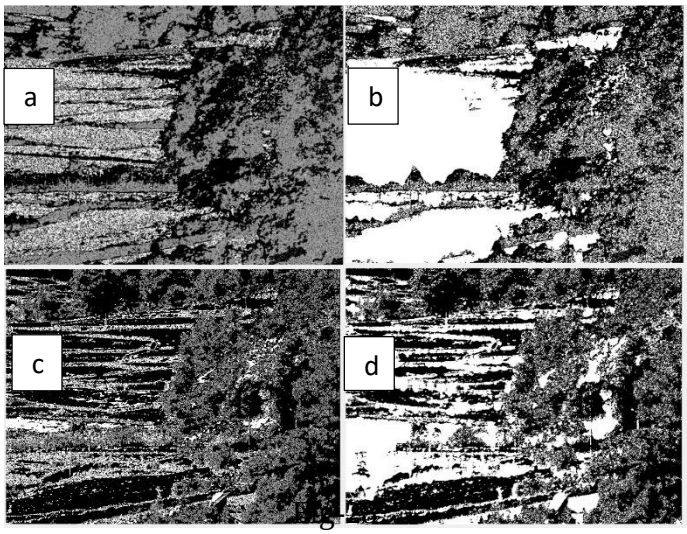

Fig-29

Fig-33a) sas,sds,scs+2 window, b) sas,sds,scs+2 window+Floyd, c) reg+sas,sds,scs+2 window, d) sas,sds,scs+2 window+ Floyd. Fig34- a) sas,sds,scs+3 window, b) sas,sds,scs+3 window+Floyd, c) reg+sas,sds,scs+3 window, d) reg+sas,sds,scs+3 window+ Floyd.

Test result 2

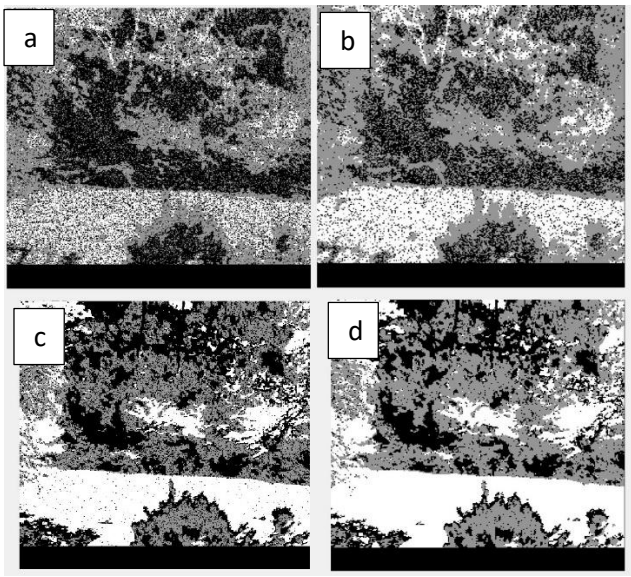

Fig-30

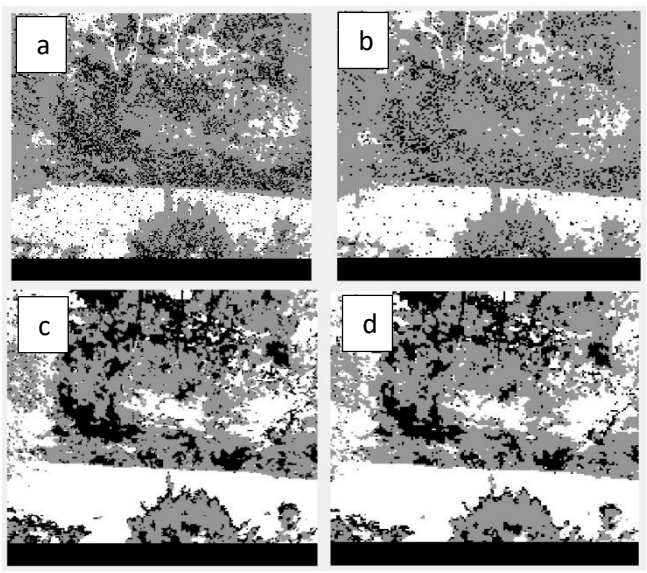

Fig-31

Fig- a) sas,sds,scs+2 window, b) sas,sds,scs+3 window, c) reg+sas,sds,scs+2 window, d) sas,sds,scs+3 window. Fig- a) sas, sds, scs+4 window, b) sas, sds,scs+5 window, c) reg+sas,sds,scs+4 window, d) reg+sas,sds,scs+5 window.

Test result 3

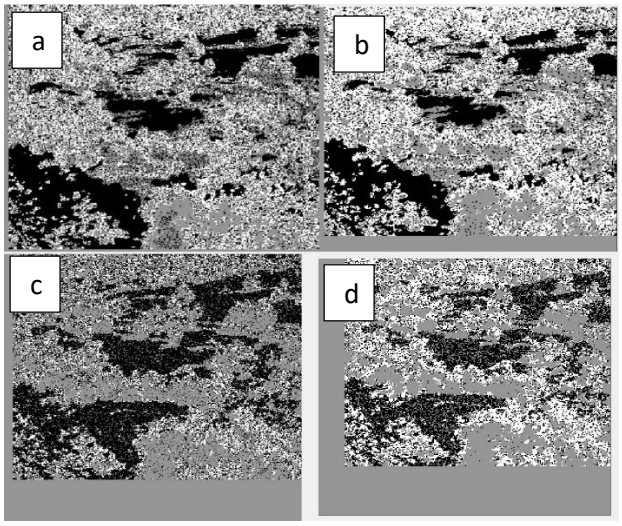

Fig-32

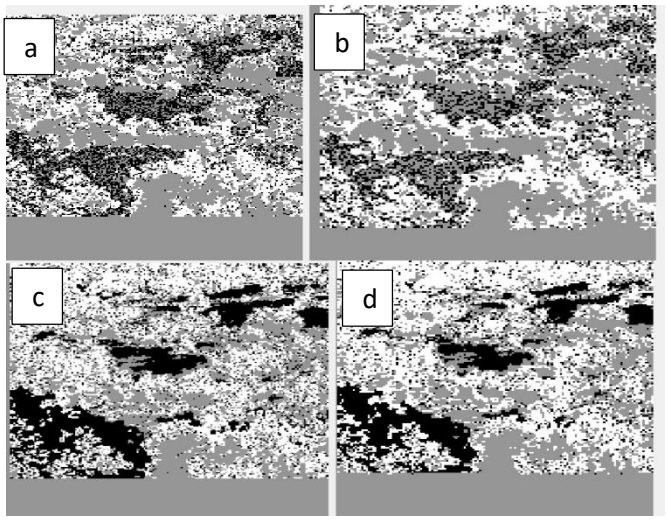

Fig-33

Fig-37 a)reg+ sas,sds,scs+2 window, b) reg+sas,sds,scs+3 window, c) sas,sds,scs+2 window, d) sas,sds,scs+3 window. Fig-38 a)reg+ sas, sds, scs+4 window, b)reg+ sas, sds,scs+5 window, c) sas,sds,scs+4 window, d) sas,sds,scs+5 window.

Test result 4- satellite hyperspectral imagery used from [101]

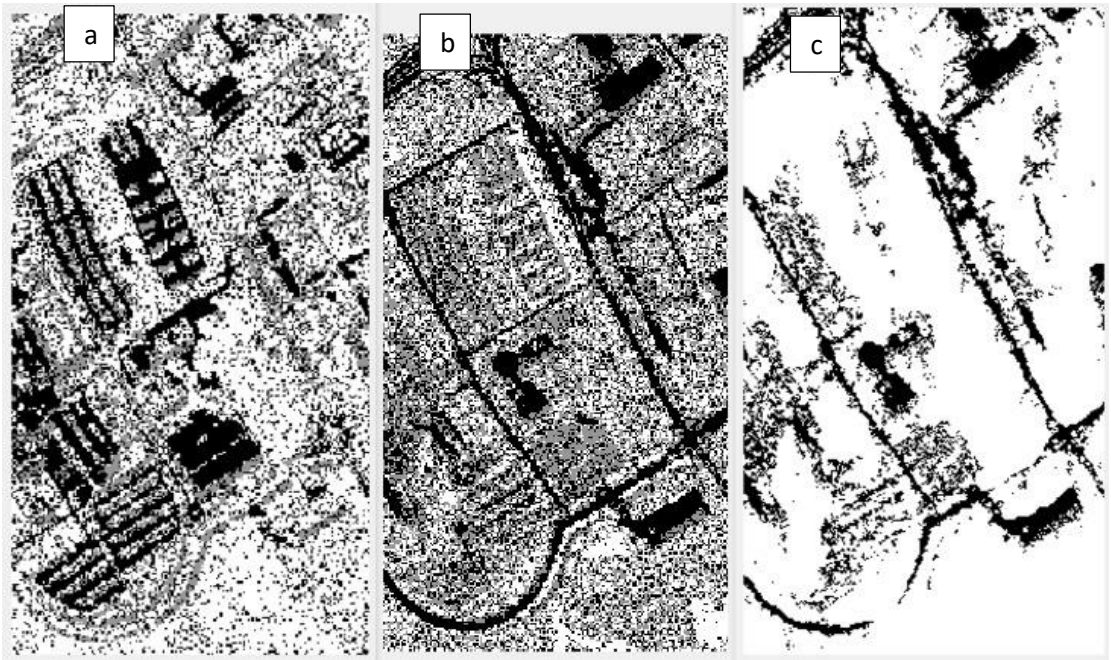

Fig-34 a) sas, sds, scs+2 window, b) reg+sas, sds, scs+2 window, c) reg+sas, sds, scs+2 window+Floyd.

4.4. Evaluation metrics

For machine learning and deep learning applications, accuracy is not an efficient metric for evaluation of the performance. There are certain other metrics are used which are described below:

4.4.1 Confusion matrix

It is a matrix that describes the performance of any classification system. For confusion matrix *C*, any element $C_{i,j}$ will represent the number of observations known to be in group *i* but classified or predicted to be in class *j*. The confusion matrix is a square matrix that show the count value of the true positive, false positive, true negative and false negative.

Consider the case of simple binary classification where only two classes exist: positive class denoted by P and negative class denoted by N. Confusion matrix for this case can be shown as below:

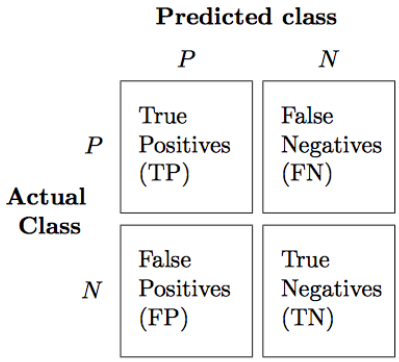

Figure :35 Confusion matrix

Note:

For multiclass classification problem, as like the case here, the value of TP, TN, FP and FN can be extracted from the confusion matrix as below:

- For any class, total number of examples will be the sum of the corresponding row (*i.e.* TP + FN)
- For any class, total number of FN will be the sum of values in the corresponding row (excluding TP) while FP will be the sum of values in the corresponding column (excluding TP)

- For any class, total number of TN will be the sum of rows and columns (excluding the row and column corresponding to that class)

4.4.2 Precision

It denotes the fraction of prediction which actually have positive class out of the total positive predicted classifications.

$$PRE = \frac{True\ Positives}{Predicted\ Positives} = \frac{TP}{TP + FP}$$

4.4.3 Recall

It denotes that of all the samples having positive class, what fraction correctly classified as positive class.

$$REC = \frac{True\ Positives}{Actual\ Positives} = \frac{TP}{TP + FN}$$

4.4.4 F1-score

For any classifier, precision and recall should be high. But both the precision and recall can't be high at the same time. Thus, another parameter is used for the analysis called F1-score.

$$F1 = 2\frac{PRE\ \times REC}{PRE + REC}$$

Value of F1-score lies in the range 0 to 1.

4.4.5 Accuracy

It is defined as the ratio of number of correct predictions to the total number of predictions.

$$ACC = \frac{TP + TN}{TP + TN + FP + FN}$$

4.5 Confusion matrix Results

4.5.1 Confusion Matrix

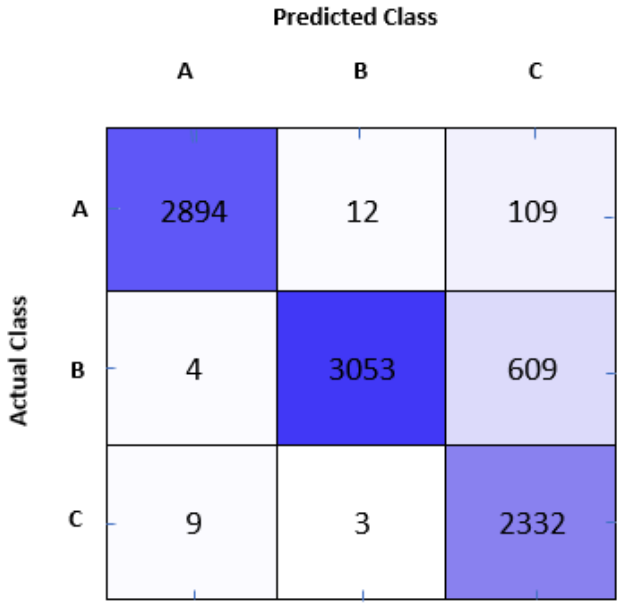

Fig 36

4.5.2 Precession, Recall and F1-score

	Precision	Recall	F1-score
Class A	0.995	0.959	0.976
Class B	0.995	0.832	0.906
Class C	0.764	0.994	0.863

4.5.3 Accuracy

Accuracy of the proposed classification algorithm is **91.73 %** (as calculated from the formula shown above)

REFERENCES

[1] R. B. Singer and T. B. McCord, “Mars: Large scale mixing of bright and dark surface materials and implications for analysis spectral reflectance,” in Proc. 10th Lunar Planatery Science Conference, pp. 1835 – 1848, 1979.

[2] B. Hapke, “Bidirectional reflectance spectroscopy 1. theory,” Journal of Geophysical Research, vol. Vol. 86, No. B4, pp. 3039–3054, April 10, 1981

[3] J. M. Nascimento and J. M. Bioucas-Dias, “Nonlinear mixture model for hyperspectral unmixing,” Proc. SPIE 7477, Image and Signal Processing for Remote Sensing XV, 7477OI, pp. 7477OI1–8, 2009.

[4] N. Dobigeon, L. Tits, B. Somers, Y. Altmann, and P. Coppin, “A comparison of nonlinear mixing models for vegetated areas using simulated and real hyperspectral data,” IEEE Jouranl of Selected Topics in Applied Earth Observations and Remote Sensing, vol. 7, no. 6, pp. 1869 – 1878, 2014.

[5] B. Somers, L. Tits, and P. Coppin, “Quntifying nonlinear spectral mixing in vegetated areas: Computer simulation model validation and first results,” IEEE Jouranl of Selected Topics in Applied Earth Observations and Remote Sensing, vol. 7, no. 6, pp. 1956 – 1965, 2014

[6] R. Heylen and P. Scheunders, “A distance geometric framework for nonlinear hyperspectral unmixing,” IEEE Jouranl of Selected Topics in Applied Earth Observations and Remote Sensing, vol. 7, no. 6, pp. 1879 – 1888, 2014

[7] P. Johnson, M. Smith, S. Taylor-George, and J. Adams, “A semiempirical method for analysis of the reflectance spectra of binary mineral mixtures,” Journal of Geophysical Research, vol. 88, pp. 3557 – 3561, 1983.

[8] M. O. J. P. E. Adams, J. B.; Smith, “Spectral mixture modeling - a new analysis of rock and soil types at the viking lander 1 site,” Journal of Geophysical Research, vol. vol. 91, pp. pp. 8098–8112, 1986.

[9] J. Bioucas-Dias and et al., “Hyperspectral unmixing overview: Geometrical, statistical, and sparse regression-based approaches,” IEEE J. Sel. Topics Appl. Earth Observ., vol. 5, no. 2, pp. 354 –379, 2012

[10] W.-K. Ma and et al., “A signal processing perspective on hyperspectral unmixing: Insights from remote sensing,” IEEE Signal Process. Mag., pp. 67–81, 2014.

[11] A. D. Stocker and A. P. Schaum, “Application of stochastic mixing models to hyperspectral detection problems,” Proc. SPIE, vol. 3071, pp. 47–60, 1997.

[12] M. T. Eismann and R. C. Hardie, “Initialization and convergence of the stochastic mixing model,” Proc. SPIE, Imaging Spectrometry IX, vol. 5159, pp. 307–318, 2003.

[13] Saeid Homayouni, Michel Roux HYPERSPECTRAL IMAGE ANALYSIS FOR MATERIAL MAPPING USING SPECTRAL MATCHING

[14] —, "Distance metrics and band selection in hyperspectral processing with applications to material identification and spectral libraries," IEEE Trans. Geosci. Remote Sens., vol. 42, no. 7, pp. 1552–1565, 2004.

[15] Hybrid Bayesian Classifier for Improved Classification Accuracy Uttam Kumar, Student Member, IEEE, S. Kumar Raja, Chiranjit Mukhopadhyay, and T. V. Ramachandra, Senior Member, IEEE

[16] Hyperspectral image processing and analysis B. Krishna Mohan* and Alok Porwal Centre of Studies in Resources Engineering, Indian Institute of Technology (Bombay), Mumbai 400 076, India

[17] HYPERSPECTRAL IMAGE ANALYSIS FOR MATERIAL MAPPING USING SPECTRAL MATCHING Saeid Homayouni, Michel Roux GET – Télécom Paris – UMR 5141 LTCI - Département TSI {saeid.homayouni, michel.roux}@enst.fr 46 rue Barrault, 75013 Paris, France

[18] SUnGP: A greedy sparse approximation algorithm for hyperspectral unmixing Naveed Akhtar, Faisal Shafait and Ajmal Mian School of Computer Science and Software Engineering The University of Western Australia WA, 35 Stirling Highway, Crawley, 6009

[19] (http://aviris.jpl.nasa.gov/data/free data.html)

[20] M. D. Iordache, J. B. Dias, and A. Plaza. Sparse unmixing of hyperspectral data, IEEE Trans. Geosci. Remote Sens., vol. 49, no. 6, pp. 2014 - 2039, 2011.

[21] Z. Shi, W. Tang, Z. Duren, and Z. Jiang, Subspace Matching Pursuit for Sparse Unmixing of Hyperspectral Data, IEEE Trans. Geosci. Remote Sens., vol. PP, no. 99, pp. 1-19, 2013.

[22] Multiple Feature Learning for Hyperspectral Image Classification Jun Li, Xin Huang, Senior Member, IEEE, Paolo Gamba, Fellow, IEEE, José M. Bioucas-Dias, Member, IEEE, Liangpei Zhang, Senior Member, IEEE, Jón Atli Benediktsson, Fellow, IEEE, and Antonio Plaza, Senior Member, IEEE

[23] http://lesun.weebly.com/hyperspectral-data-set.html

[24]http://personalpages.manchester.ac.uk/staff/d.h.foster/Hyperspectral_images_of_natural_scenes_02.html

[25] http://lesun.weebly.com/hyperspectral-data-set.html